3. Cs_2MX_4 Groups Forming no IC Phase - Temperature Dependences of Covalency between Ions in β-K_2SO_4-type Cs_2ZnX_4 (X = Cl, Br and I) and Sr_2GeS_4-type Cs_2MI_4 (M = Cd and Hg) Crystals -

3.1 Introduction

A_2BX_4-family compounds containing with isolated tetrahedral BX_4^{2-} ions, form the modification-B with monoclinic Sr_2GeS_4-type ($P2_1/m$, $Z = 2$) as shown in Fig. 3. 1 or the modification-A with orthorhombic β-K_2SO_4-type ($Pnma$, $Z = 4$) structures in Fig. 2. 7 (a). Some of modification-B compounds transform to modification-A so-called the α-β transition at a temperature $T_{\alpha\text{-}\beta}$ [1-7]. Below $T_{\alpha\text{-}\beta}$, the modification-B is more stable but often the modification-A can exist as a metastable state [8].

It has been reported that obtained crystals can be grouped into the two kinds of studies, Sr_2GeS_4- and β-K_2SO_4-type from the ratio of anionic to cationic radius (R_{MX4} / R_A) in crystals as shown in Table 3.1. Crystals can be classified into four groups closely concerning with the ratio R_{MX4} / R_A: Groups I and II given in Table 3. 1 are Sr_2GeS_4-type (modification-B) compounds without and with α-β transitions, respectively. Group III is β-K_2SO_4-type (modification-A) compounds with IC phase transitions. Group IV has the β-K_2SO_4-type structure but with no IC phase. In compounds shown in Table 3. 1, Tl and Rb salts with ZnI_4^{2-} and CoI_4^{2-} anions are classified into different groups and show large differences in transition temperatures, though Tl^+ and Rb^+ ions have close ion radii 1.64 and 1.66 Å, respectively. Its reason seems to be explained by differences in weight or ionicity of cations. In Cs salts, however, transition temperatures cannot be interpolated from those in Rb and Tl salts though Cs^+ ions have an intermediate weight

between those in Rb and Tl. This rsult implies that the ionicity of cations, i.e., the covalency of interionic bonds, play an important role in the phase transition sequence of A_2BX_4 compounds.

Table 3. 1 Crystal structures, ionic ratios and transition temperatures in A_2BX_4 family compounds

Group	A_2BX_4	structure	R_{MX4}/R_A	T_{tr} / K	$T_{\alpha-\beta}$/ K	T_{IC} / K	T_C / K	ref.
	K_2ZnI_4	Sr_2GeS_4	3.092	270	–			[6]
I	K_2CoI_4		3.066	250	–			[7]
	Tl_2ZnI_4		2.866	209	–			[9]
	Tl_2CoI_4		2.841	192	–			[10]
	K_2ZnBr_4	Sr_2GeS_4	2.809	155	~470	561	291	[1]
	K_2CoBr_4		2.750	143	~470	553	303	[2]
	Rb_2ZnI_4		2.831	62.4	~530	unknown	unknown	[3]
II	Rb_2CoI_4		2.807	30	~515	unknown	unknown	[4]
	Tl_2ZnBr_4		2.604	18	~480	455	unknown	[5]
	Tl_2CoBr_4		2.549	18	~480	445	unknown	[5]
	Cs_2CdI_4		2.691	–	~420	332	259	[11]
	Cs_2HgI_4		2.691	–	~510	255	200	[12]
	K_2ZnCl_4	β-K_2SO_4	2.612			553	403	[13]
	Rb_2ZnBr_4		2.572			347	192	[13]
	Rb_2CoBr_4		2.518			333	193	[14]
	Tl_2ZnCl_4		2.421			363	173	[15]
	Rb_2ZnCl_4		2.392			303	192	[13]
III	Rb_2CoCl_4		2.337			295	192	[14]
	Cs_2CdBr_4		2.453			252	237	[13]
	Cs_2HgBr_4		2.453			243	230	[13]
	Cs_2HgCl_4		2.287			219	183	[16]
	K_2SeO_4		2.026			129.5	93	[13]
	Cs_2ZnI_4		2.597			117	108	[17]
IV	Cs_2ZnBr_4	β-K_2SO_4	2.359			–	–	[18]
	Cs_2ZnCl_4		2.193			–	–	[19]

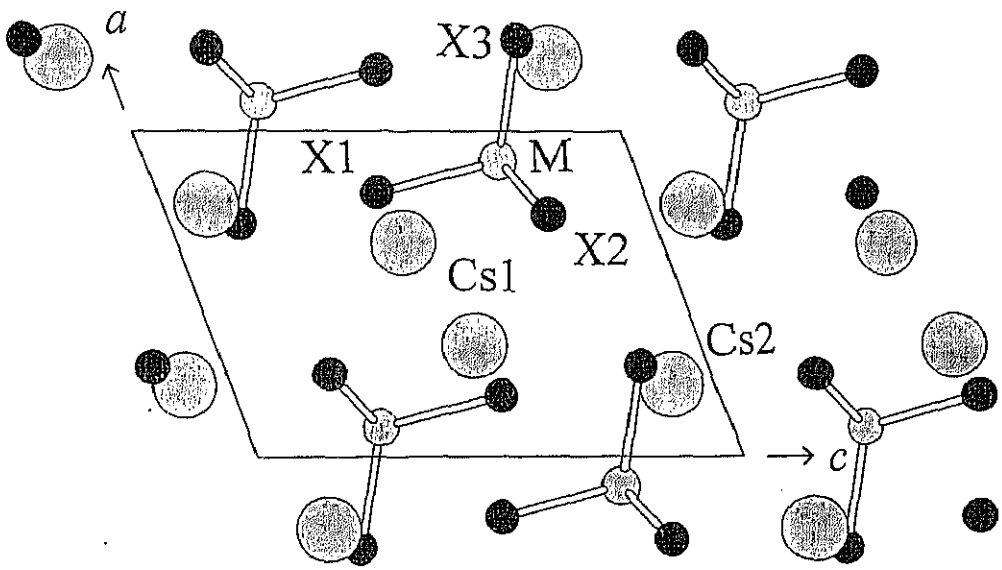

Fig. 3. 1 Crystal structure in A_2BX_4 with the Sr_2GeS_4-type structure ($P2_1/m$, $Z = 2$) projected on *ac*-plane.

It has been reported that so-called ionic crystals do not consist of purely isolated ions but involve covalency to some extent even in alkali halides [20, 21]. From the calculation by using electronegativities, degrees of covalency between Na^+ and Cl^- ions in NaCl crystals can be estimated from methods by Pauling (0.332 [22]) and Sanderson (0.334 [21]). The difference in covalency between ions in β-K_2SO_4-type (modification-A) and in Sr_2GeS_4-type (modification-B) compounds is, therefore, worthy of remark as a reason why some of β-K_2SO_4-type compounds undergo N-IC phase transitions but all Sr_2GeS_4-type compounds have no IC phase. Since the covalency between ions markedly influences to the electric field gradient at nuclei in these ions, the measurement of quadrupolar perturbed NMR spectra is considered to be quite a suitable probe for the investigation of covalency [23]. As another information obtainable from NMR spectra, chemical shift is also sensitive to the total degree of covalency[24, 25]. In the present study, Cs_2ZnCl_4, Cs_2ZnBr_4, Cs_2ZnI_4, and modification-Bs of Cs_2CdI_4 and Cs_2HgI_4 without phase transitions below room temperature are taken up and NMR spectrum and spin-lattice relaxation time T_1 measurements for quadrupolar nuclei ^{133}Cs are performed on these compounds in order to clarify the effect caused by structure difference.

3.2 Theory

3.2.1 ^{133}Cs NMR spectra

3.2.1(a) Frequency shift caused by second order perturbation of nuclear quadrupole interaction

The first order perturbation from electric field gradient on ^{133}Cs NMR mentioned in section 2. 2. 2 causes shifts for the single quantum transitions $m \Leftrightarrow m$ -1 except for the central transition 1/2 $\Leftrightarrow$ -1/2. On the other hand, the second order effect appears only as a smaller shift of the central transition. To determine the exact chemical shift value from the quadrupolar perturbed NMR spectrum, this second order shift has to be taken into account. For powder specimens, the second order perturbation causes both line broadening and shift. The frequency of the main peak can be given by [26]

$$\nu^{(2)} = -\frac{\nu_Q^2}{12\nu_L}\left[I(I+1)-\frac{3}{4}\right]\left[1+\frac{\eta^2}{3}\right], \qquad (3.5)$$

where $\nu_L=\omega_L/2\pi$, I and η are Larmor frequency, the nuclear spin in question and the asymmetric parameter, respectively, and ν_Q is represented by $\nu_Q \equiv 3e^2Qq/2I(2I-1)h$. For a ^{133}Cs nucleus, the second order shift is given by

$$\nu^{(2)} = -\frac{5(e^2Qq/h)^2}{784\nu_L}\left[1+\frac{\eta^2}{3}\right]. \qquad (3.6)$$

In case e^2Qq/h=300 kHz, η =0 and ν_L =39.4, the central peak shift is *ca.* 15 Hz in the

low-frequency side.

3.2.1(b) Relations between chemical shift and the total degree of covalency in ionic bonds

The chemical shift of an NMR absorption line, or the shielding constant, is expressed as $\sigma = (\nu_{sample} - \nu_{naked}) / \nu_{naked}$ where ν_{sample} and ν_{naked} are resonance frequencies of the sample and a naked nucleus, respectively, both at constant magnetic fields. The shielding tensor was formulated by Ramsey in the first approximation as [27]

$$\tilde{\sigma} = \tilde{\sigma}_D + \tilde{\sigma}_P$$

$$= -\frac{e^2}{3mc^2}\left\langle 0\left|\sum_j r_j^{-1}\right|0\right\rangle$$

$$+\frac{2}{3}\left(\frac{e\hbar}{2mc}\right)^2 \sum_n \frac{1}{E_n - E_0}\left\{\left\langle 0\left|\sum_j L_j\right|n\right\rangle\left\langle n\left|\sum_j L_j r^{-3}\right|0\right\rangle + \left\langle 0\left|\sum_j L_j r_j^{-3}\right|n\right\rangle\left\langle n\left|\sum_j L_j\right|0\right\rangle\right\}, \quad (3.7)$$

where e, m and L_j are the charge and mass of an electron and the orbital angular momentum, respectively, r_j is the distance between the jth electron and the nucleus, E_0 and E_n are energies of the electronic ground state and the nth excited state, respectively. Here, $\tilde{\sigma}$ represents the diagonalized tensor with diagonal components σ_{XX}, σ_{YY} and σ_{ZZ}. The first term in the shielding tensor $\tilde{\sigma}_D$ called the diamagnetic term is related only to the electron density around the atomic nucleus in question. The paramagnetic term $\tilde{\sigma}_P$ indicates that the local field which is induced by electron transfer between the ground and excited states. The experimental chemical shift is observed relatively as the

difference from that of the reference sample, because the shift of the naked nucleus is unavailable. Taking into account the relative chemical shift, the paramagnetic term in heavy atoms is about two orders of magnitude larger than the diamagnetic one, which is inappreciably different between in various compounds, implying that the paramagnetic terms dominant in heavy atoms [28]. Thus, only the paramagnetic term will be taken into account for the interpretation of ^{133}Cs NMR chemical shift in the following discussion. In what follows, approximate discussion using the isotropic shielding constant $\sigma = (\sigma_{XX} + \sigma_{YY} + \sigma_{ZZ})/3$ will be employed because of a great difficulty for taking into account all diagonal components. When the covalency of the bond is small enough to permit to consider a pair of atom in the bonding as an isolated system, the isotropic relative shielding constant in a halogen nucleus relative from the ideal ion is given by [24]

$$\sigma = \lambda \frac{2e^2\hbar^2}{3m^2c^2} \frac{1}{\Delta E} \left\langle \frac{1}{r^3} \right\rangle_p , \tag{3.8}$$

where λ is the total bond covalency (conversely, (1-λ) is the bond ionicity), ΔE the mean energy of all excited states contributing to the probability, and $\langle 1/r^3 \rangle_p$ the mean $1/r^3$ values of a valence p-electron making the partial covalency in an ionic bond. Furthermore, Yoshida and Moriya gave shielding constants in halogen and metal nuclei for metal halide crystals in more detail as [25]

$$\sigma_X = \frac{2e^2\hbar^2}{3m^2c^2} z \frac{b^2}{\Delta E'^2} \frac{1}{\Delta E} \left\langle \frac{1}{r^3} \right\rangle_{p,X} \tag{3.9}$$

and

$$\sigma_M = \frac{2e^2\hbar^2}{3m^2c^2} a_p^2 z \frac{b^2}{\Delta E'^2} \frac{1}{\Delta E} \left\langle \frac{1}{r^3} \right\rangle_{p,M}, \tag{3.10}$$

respectively, where b^2 means $\left(\langle 0|V_t|n\rangle\right)^2$ where V_t is the Hamiltonian transfering an electron of the halogen ion into a neighboring metal ion, z is the coordination number, $\mu_B = e\hbar/2m$ is Bohr magneton and a_p is the fraction of p-orbitals related to hybrid orbitals in the partial-covalent bond. ΔE' and ΔE are energies of the states with and without covalent bonding [25]. Therefore ΔE' is generally smaller than ΔE. Since $b^2/\Delta E'^2$ represents the degree of covalency λ' in a single bond, $zb^2/\Delta E'^2$ is equal to the total degree of covalency λ. For ^{133}Cs, eq. (3.10) is rewritten as

$$\sigma_{Cs} = \lambda \frac{2e^2\hbar^2}{3m^2c^2} \frac{1}{\Delta E} \left(a_p^2 \left\langle \frac{1}{r^3} \right\rangle_p + a_d^2 \left\langle \frac{1}{r^3} \right\rangle_d + a_f^2 \left\langle \frac{1}{r^3} \right\rangle_f \right). \tag{3.11}$$

This includes contributions to chemical shifts from d- and f-orbitals caused by the partial bond covalency. Here, a_d and a_f are fraction of d- and f-orbitals related to partial-covalent bonds, and $\left\langle 1/r^3 \right\rangle_d$ and $\left\langle 1/r^3 \right\rangle_f$ are the mean values of $1/r^3$ for the valence d- and f-electron.

The lowest excited state allowed for the electron transition in metal halide is the p-state but its ΔE is not known because its transition is forbidden for optical transition [24]. Therefore, these values were anticipated from energies of s-type excited states and conduction bands by Kanda[24] to be ca. 8, 7 and 6 eV for chloride, bromide and iodide in the same order. Yoshida and Moriya assumed a relation in NaCl and CsCl type cubic structures as [25]

$$\Delta E = \frac{(2\alpha - 1)e^2}{R} + E_{\text{aff,X}} - E_{\text{ion, M}}, \tag{3.12}$$

where R means the interionic distance, α is the Madelung constant, i.e., the first term corresponds to the cohesive energy in an ionic crystal [21], $E_{\text{aff,X}}$ is the electron affinity of the halogen and $E_{\text{ion,M}}$ is the ionization potential of the metal. Since for crystals of intricate structure such as β-K_2SO_4 type, Madelung constants have not been known, the semi-empirical lattice energy U_{ion} derived by Kapustinskii given by [21]

$$U_{ion} = 12.44 \frac{n z_+ z_-}{r_+ + r_-}\left(1 - \frac{0.345}{r_+ + r_-}\right) \tag{3.13}$$

is usually employed, where n, r and z are the number of ions contained in chemical formula, ionic radii and formal charges, respectively, in which indices + and - represent cation and anion in the same order. Equation (3.13) is taken account into the Born-Mayer repulsion potential given as [21]

$$U_{rep} \propto \exp(-R / 0.345). \qquad (3.14)$$

More exactly, the first term in eq. (3.12) should be multiplied by the term taken into account the repulsion potential (1 - 0.345/*R*). Using the $\langle 1/r^3 \rangle_p$ values given by Barnes and Smith[29] and the mean exited energy ΔE introduced by Yoshida and Moriya [25], the total degrees of covalency of halogen ions in metal halides was estimated by Yoshida and Moriya[25] as listed in Table 3. 1. In real crystals, quantitative determination of λ is difficult, because values of ΔE and $\langle 1/r^3 \rangle$ for intricate hybrid orbitals in the complex molecules can not be accurately determined.

Table 3. 2 Total covalencies λ of halogen ions estimated from reported values of chemical shifts [24], ΔE taking into account the Born-Mayer repulsion potensial and reported values $\langle 1/r^3 \rangle_p a_0^3$ [29] in metal halides with the CsCl- and the NaCl-type cubic structures.

Compound	Crystal structure	σ/ppm	ΔE / eV	$\langle 1/r^3 \rangle_p a_0^3$	λ / %
TlCl	CsCl	251	7.52	7.16	27
TlBr	CsCl	620	6.96	13.55	33
AgBr	NaCl	189	7.97	13.55	12
LiBr	NaCl	89.6	9.56	13.55	7
KI	NaCl	148	8.00	18.0	7

3.2.2 Thermal expansion of crystal lattice

Thermal expansion of crystal lattice is an important property closely related to anharmonicity of lattice vibrations especially in high-temperature region. Considering simple monoatomic solid, the atomic potential U in the vicinity of equilibrium position is represented as

$$U = \frac{1}{2}ax^2 - \frac{1}{3}bx^3 - \cdots,$$

where x is the displacement from the potential minimum position r_0, and a and b are constants. The first and second terms indicate harmonic and anharmonic contributions, respectively. Ignoring terms higher than the 4th order, the coefficient of linear expansion is expanded as

$$\alpha = \frac{kb}{a^2 r_0},$$

where k is the Boltzman constant. Therefore, if the constant b =0, i.e., the term of x^3 vanishes, crystal lattices do not expand thermally. The averaged coefficients of linear and cubic expansions are defined to be

$$\overline{\alpha}_i = \frac{1}{L_i(T_0)}\left(\frac{L_i(T) - L_i(T_0)}{T - T_0}\right)_p \tag{3.15}$$

and

$$\overline{\alpha}_V = \frac{1}{V(T_0)}\left(\frac{V(T)-V(T_0)}{T-T_0}\right)_p, \tag{3.16}$$

respectively, where index $i = x, y, z$, $L(T)$ and $V(T)$ are unit lattice constants and the volume at a temperature T, respectively, and T_0 is the reference temperature. Thus, at the limit $\Delta T = T - T_0 \rightarrow 0$, the coefficients of thermal expansions α_i and α_V are, respectively, rewritten as [30]

$$\alpha_i = \lim_{\Delta T \to 0} \overline{\alpha}_i = \frac{1}{L_i(T_0)}\left(\frac{\partial L_i(T)}{\partial T}\right)_p \tag{3.17}$$

and

$$\alpha_V = \lim_{\Delta T \to 0} \overline{\alpha}_V = \frac{1}{V(T_0)}\left(\frac{\partial V(T)}{\partial T}\right)_p. \tag{3.18}$$

One-third values of coefficients of cubical expansion ($\alpha_V/3$) in various solid state compounds are listed in Table 3.2.

Table 3. 3 One-third of averaged coefficients of cubical expansion ($\overline{\alpha}_V$ /3) in various inorganic compounds [31-37].

Compound	Temperature / ℃	($\overline{\alpha}_V$ /3) / 10^{-6} K^{-1}	Compound	Temperature / ℃	($\overline{\alpha}_V$ /3) / 10^{-6} K^{-1}
AgCl	20 ~ 150	34.3	$KMnO_4$	-78 ~ 18	73.3
Al_2O_3	20 ~ 800	2.67	KNO_3	-78 ~ 18	70.0
$BaCl_2$	20 ~ 150	20.0	KOH	30 ~ 130	65.3
$BaZrO_3$	25 ~ 1402	7.57	K_2SO_4	-78 ~ 21	43.3
$CaCl_2$	20 ~ 150	22.3	$KTaO_3$	20 ~ 327	9.8
CaO	30 ~ 75	21.0	MgO	30 ~ 75	13.3
$CaTiO_3$	20 ~ 900	12.9	NaCl	-79 ~ 0	36.7
$CaZrO_3$	25 ~ 1402	10.4	NaOH	20 ~ 120	28.0
KBr	-79 ~ 0	40.0	$NaNbO_3$	20 ~ 200	11.0
KCl	-78 ~ 25	36.7	$PbTiO_3$	27 ~ 490	-5.33
$KClO_3$	-78 ~ 21	73.3	$PbTiO_3$	490 ~ 535	8.33
KI	-79 ~ 0	41.7	$SrTiO_3$	27 ~ 1727	10.8

3.3 Cesium tetrachlorozincate Cs_2ZnCl_4

3.3.1 Introduction

Cesium tetrachlorozincate Cs_2ZnCl_4 forms colorless crystals with orthorhombic β-K_2SO_4 structure (space group *Pnma* Z = 4) at room temperature. Three ^{35}Cl NQR signals with an intensity ratio 2:1:1 [38] which agrees with the ratio of nonequivalent Cl sites in the structure determined at room temperature [39] were reported. Cs_2ZnCl_4 undergoes a transition at T_{tr} = 572 K [40] and melts at T_m = 837 K [41], but the structure of the high-temperature phase has not been reported. The dielectric constant along *b*-axis has been reported to show a broad maximum around *ca.* 80 K[41] and a large anomaly at 572 K[40]. A specific heat measurement also showed an anomaly at 572 K due to the phase transition [40]. The X-ray intensity from (8 0 0) diffraction decreases critically with temperature increase up to 572 K [40].

3.3.2 Experimental

Crystals of Cs_2ZnCl_4 with the β-K_2SO_4 structure was grown by cooling a molten mixture containing stoichiometric amounts of CsCl (purity 99.9%) and $ZnCl_2$ (purity 99.9%) purchased from Wako Pure Chemical Industries, Ltd. The obtained crystalline powder was dried *in vacuo* and then sealed in glass tubes with nitrogen gas for DTA and NMR measurements.

Differential thermal analysis (DTA) was carried out to confirm reported phase transitions found in a range 100-300 K. The sample temperature was determined within $\pm$0.2 K by using a chromel-constantan thermocouple.

To confirm lattice parameters, X-ray powder diffraction was measured and

their temperature dependences were obtained using a Phillips X'Pert PW3050/00 diffractometer in a range 180-360 K.

The ^{133}Cs NMR spectra were measured with a Bruker MSL-300 NMR system at a Larmor frequency of 39.4 MHz in a range 210-362 K. A saturated CsCl aqueous solution was used as a standard of frequency shift and the setting the pulse width. All ^{133}Cs NMR spectra were measured by applying a single detection 90° pulse with a width 4-6 μs. ^{133}Cs NMR T_1 measurements were performed with a Bruker MSL-300 NMR system at a Larmor frequency of 39.4 MHz using the saturation-τ- 90° pulse sequence in a range 211-364 K. The sample temperature was controlled within $\pm$0.5 K with a VT-1000 temperature controller and determined by a copper-constantan thermocouple with the same accuracy. The uncertainty in the T_1 measurement was estimated to be within 5 %.

3.3.3 Result

No thermal anomaly was detected by DTA measurement between 100 and 300 K. An X-ray powder diffraction pattern observed at *ca.* 300 K is shown in Fig. 3. 2 together with diffraction lines simulated by using previously reported atomic coordinates determined at room temperature [39]. Lattice parameters determined from the obtained pattern at *ca.* 300 K given below agreed well with reported values shown in parentheses: a =9.76 Å (9.7577 Å), b =7.41 Å (7.4004 Å) and c =12.98 Å (12.9704 Å). Temperature dependeences of lattice parameters are shown in Fig. 3. 3. Lattice parameters a, b and c and the cube root of unit cell volume $V^{1/3}$ decreased with temperature decrease.

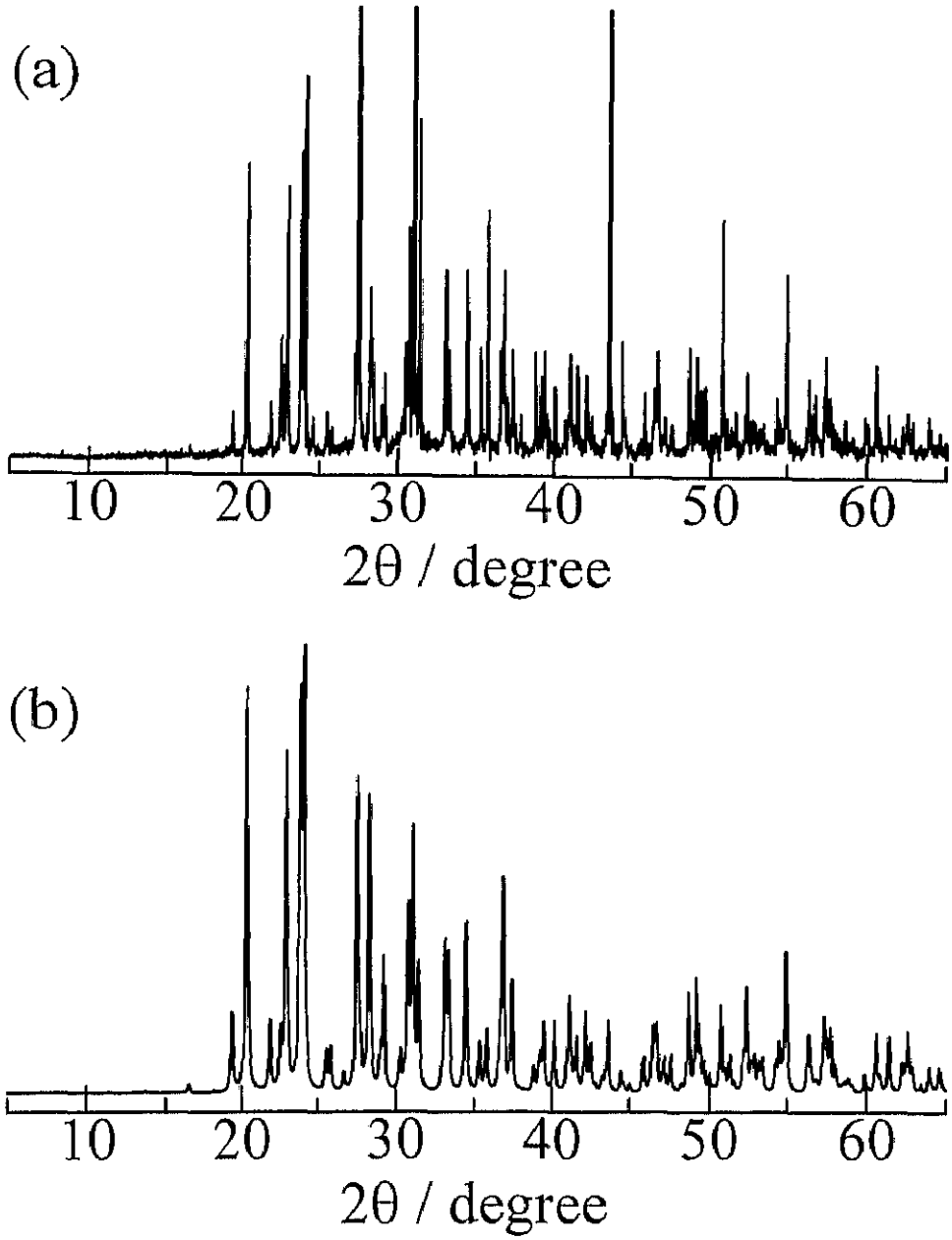

Fig. 3. 2 (a) An X-ray powder diffraction pattern observed at ca. 300 K in Cs_2ZnCl_4. (b) A simulated powder pattern using reported atomic coordinates [39].

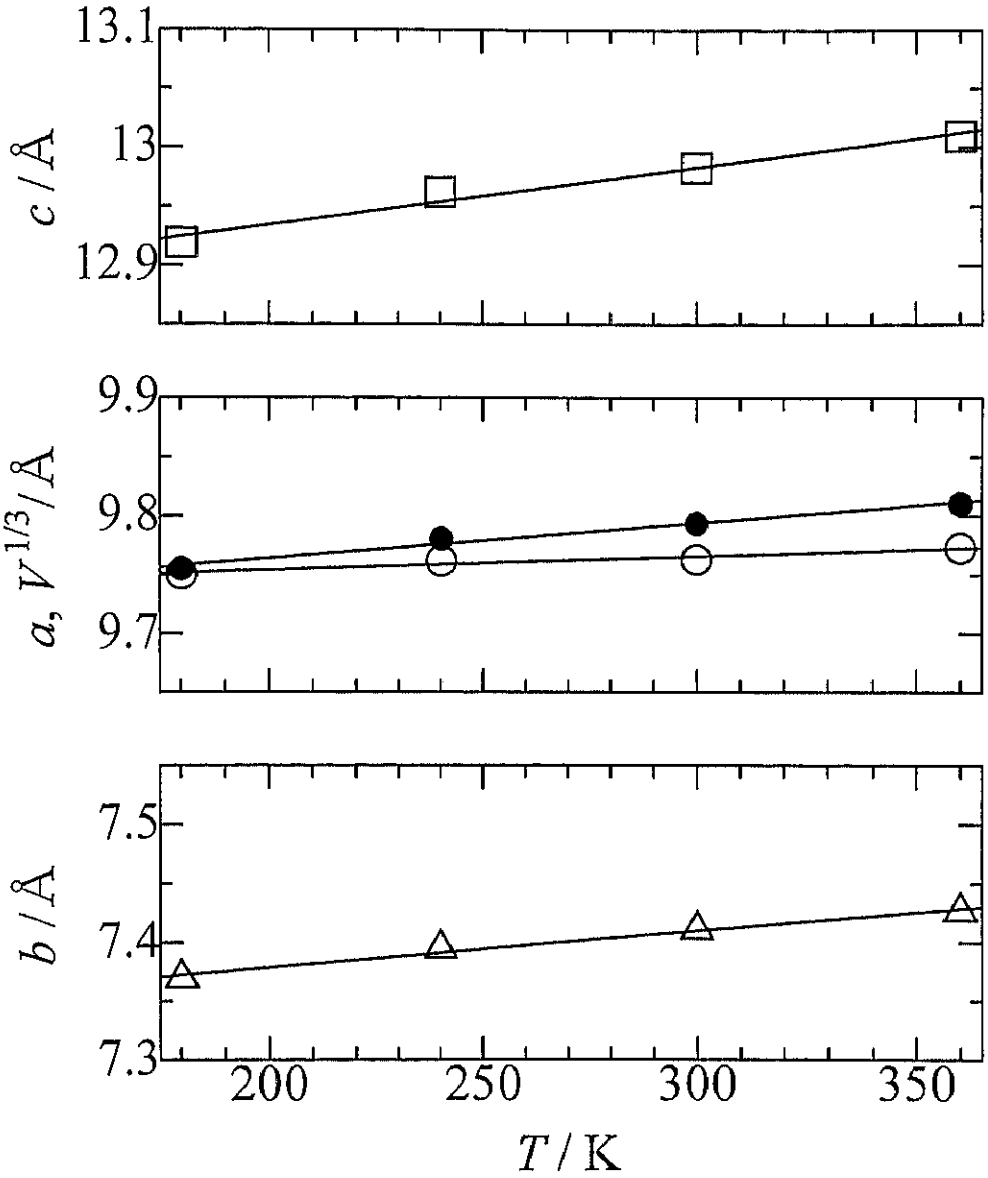

Fig. 3. 3 Temperature dependences of the lattice parameters a (○), b (△) and c (□), and the cube root of a unit cell volume $V^{1/3}$ (●) observed in Cs_2ZnCl_4.

Quadrupolar perturbed ^{133}Cs NMR spectra observed at 362, 294 and 210 K are shown in Fig. 3. 4. The width of a 90° pulse tuned for the measurement of powder sample of Cs_2ZnCl_4 was the same as that in the standard CsCl aqueous solution. This suggests that all single quantum transitions were contained in observed ^{133}Cs NMR spectra indicating that small quadrupole coupling constants (e^2Qq/h). The observed line-shapes are explainable by the superposition of two 1st order perturbed spectra. This result is consistent with the reported crystal structure containing two crystallographically nonequivalent Cs ions [39]. The estimated values of e^2Qq/h and asymmetric parameter η at 300 K were estimated to be 150±30 kHz and 0.05±0.05, and 200±70 kHz and 0.5±0.1, respectively, by referring to the values obtained from the single crystal ^{133}Cs NMR measurement in Cs_2HgBr_4 [42].

The recovery of ^{133}Cs magnetization after a 90° pulse could be reproduced by a single exponential curve in the whole temperature range studied and a unique T_1 value could be determined. Temperature dependences of ^{133}Cs NMR T_1 are shown in Fig. 3. 5. The T_1 increased with temperature decrease.

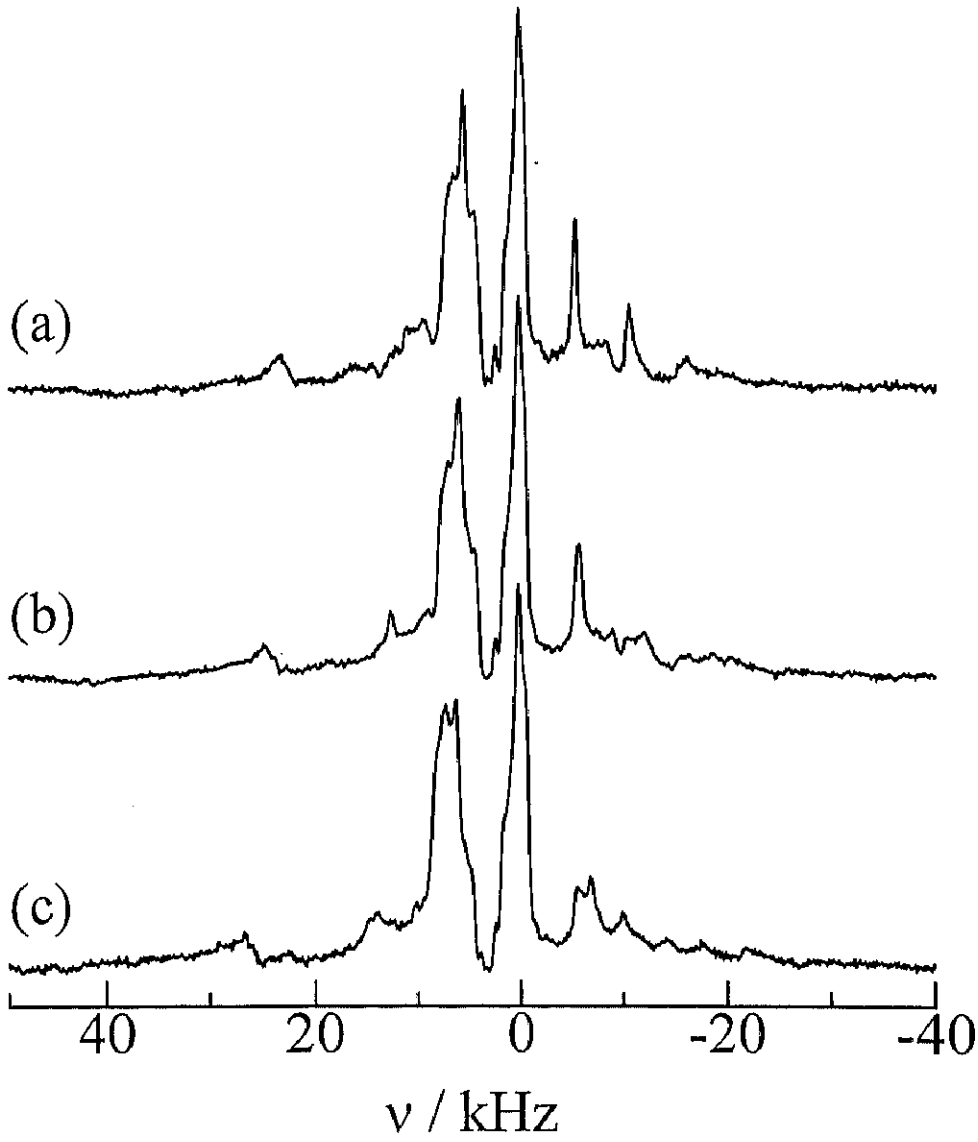

Fig. 3. 4 Quadrupolar perturbed ^{133}Cs NMR spectra measured at 39.4 MHz at 362 (a), 294 (b) and 210 K (c) in Cs_2ZnCl_4.

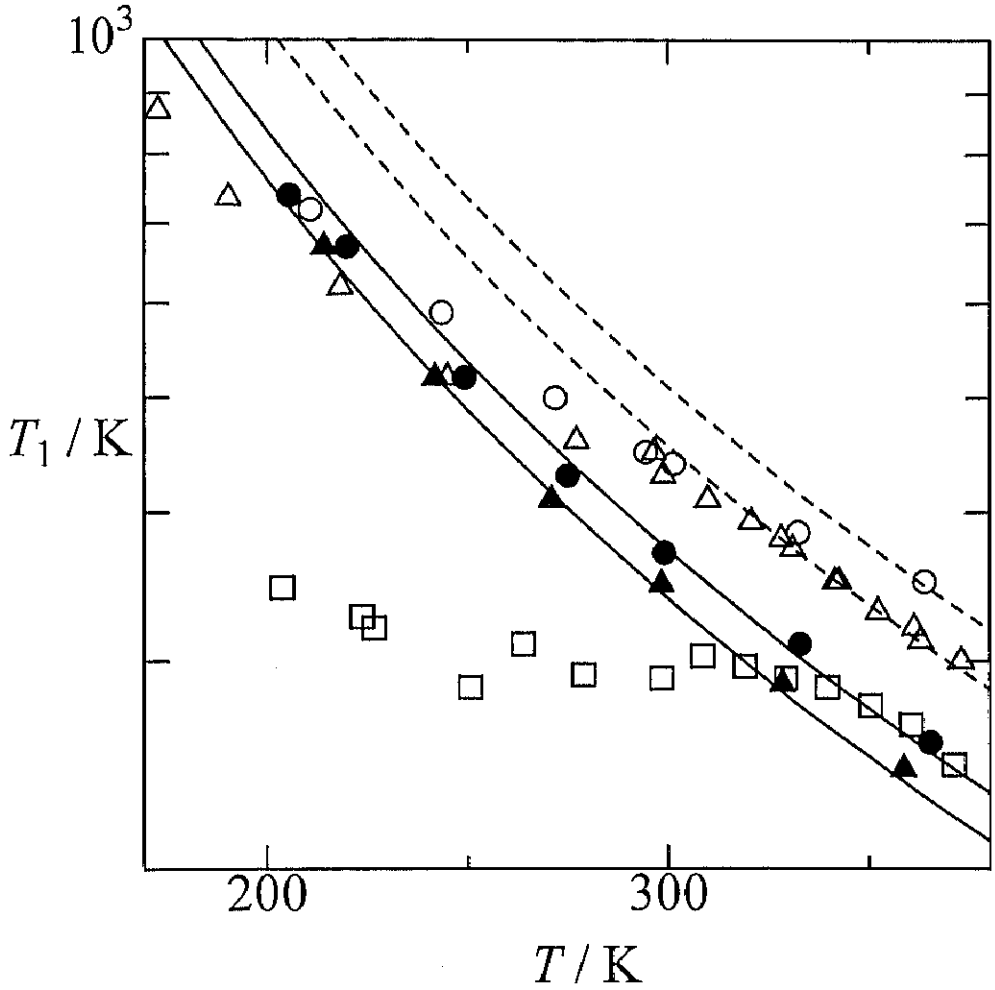

Fig. 3. 5 Temperature dependences of ^{133}Cs NMR T_1 in Cs_2ZnCl_4 (●), Cs_2ZnBr_4 (▲) and Cs_2ZnI_4 (■) with the β-K_2SO_4-type structure, and Cs_2CdI_4 (○) and Cs_2HgI_4 (△) with the Sr_2GeS_4-type. Broken and Solid lines are theoretical curves calculated by using eq. (2.6) for compounds with the former and the later structures.

3.4 Cesium tetrabromozincate Cs_2ZnBr_4

3.4.1 Introduction

Cesium tetrabromozincate Cs_2ZnBr_4 forms colorless crystals and takes an orthorhombic β-K_2SO_4 structure (space group *Pnma* $Z = 4$) at room temperature [43]. Three ^{81}Br NQR signals with an intensity ratio 2:1:1 in good agreement with the crystal structure were reported in the temperature range between 77 K and 300 K [38, 44]. From the comparison of ^{81}Br NQR spin-lattice relaxation times T_{1Q} observed for respective peaks and their temperature dependences, it was suggested that the libration of tetrahedral $ZnBr_4^{2-}$ ions about *a*-axis is further excited than around the other axes in the temperature region between 77 and 300 K [44]. No phase transiton other than melting at 850 K [41] was reported in Cs_2ZnBr_4 below 300 K down to at least 5 K from the temperature dependence of ^{81}Br NQR measurement [18]. The dielectric constant measured along *b*-axis has been reported to show a broad maximum around about 70 K but no anomaly due to a phase transition [41].

3.4.2 Experimental

Crystals of Cs_2ZnBr_4 with a β-K_2SO_4 structure were grown with cooling a molten mixture containing stoichiometric amounts of CsBr (purity 99.9%) and $ZnBr_2$ (purity 99.9%) purchased from Wako Pure Chemical Industries, Ltd. The obtained crystalline powder was dried *in vacuo* and then sealed in glass tubes with nitrogen gas for DTA and NMR measurements.

DTA was carried out to confirm reported phase transitions in a range 100-300 K. The sample temperature was determined within ±0.2 K by using a chromel-

constantan thermocouple.

To confirm lattice parameters, X-ray powder diffraction was measured and their temperature dependences were obtained using a Phillips X'Pert PW3050/00 diffractometer in a range 180-360 K.

The ^{133}Cs NMR spectra were measured with a Bruker MSL-300 NMR system at a Larmor frequency of 39.4 MHz in a range 209-368 K. A saturated CsCl aqueous solution was used as a standard of frequency shift and the setting the pulse width. All ^{133}Cs NMR spectra were measured by applying a single detection 90° pulse with a width 4-6 μs. ^{133}Cs NMR T_1 measurements were performed with a Bruker MSL-300 NMR system at a Larmor frequency of 39.4 MHz using the saturation-τ- 90° pulse sequence in a range 173-373 K. The sample temperature was controlled within ±0.5 K with a VT-1000 temperature controller and determined by a copper-constantan thermocouple with the same accuracy. The uncertainty in the T_1 measurement was estimated to be within 5 %.

3.4.3 Result

No thermal anomaly was detected by DTA measurement between 100 and 300 K. An X-ray powder diffraction pattern observed at *ca.* 300 K is shown in Fig. 3. 6 together with diffraction lines simulated by using previously reported atomic coordinates determined at room temperature [43]. Lattice parameters determined from the experimental pattern at *ca.* 300 K given below agreed well with reported values shown in parentheses: a =10.22 Å (10.196 Å), b =7.73 Å (7.770 Å) and c =13.54 Å

(13.517 Å). Temperature dependeences of lattice parameters are shown in Fig. 3. 7. Lattice parameter a increased with temperature decrease down to *ca.* 330 K and showed the maximum at *ca.* 330 K and $V^{1/3}$ showed plateau above *ca.*330 K. Both parameters a and $V^{1/3}$ decreased with temperature decrease in a range below *ca.* 330 K. Parameters b and c decreases monotonically with cooling in the whole temperature region studied.

Quadrupolar perturbed ^{133}Cs NMR spectra observed at 367, 299 and 210 K are shown in Figs. 3. 8. The width of a 90° pulse tuned for the measurement of powder samples was the same as that in the standard CsCl aqueous solution. This suggests that all single quantum transitions were contained in observed ^{133}Cs NMR spectra indicating that small ^{133}Cs quadrupole coupling constants (e^2Qq/h) . The observed line-shapes can be explained by the superposition of two 1st order perturbed spectra. This result is consistent with the reported crystal structure containing two crystallografically nonequivalent Cs ions [43]. Estimated values of e^2Qq/h and asymmetric parameter η are 120 ± 30 kHz and 0.1 ± 0.1, and 250 ± 70 kHz and 0.5 ± 0.2, respectively, by referring to the values obtained from the single crystal ^{133}Cs NMR measurement in Cs_2HgBr_4 [42].

The recovery of ^{133}Cs magnetization after a 90° pulse could be reproduced by a single exponential curve in the whole temperature range studied and a unique T_1 value could be determined. Temperature dependences of ^{133}Cs NMR T_1 are shown in Fig. 3. 5. The T_1 increased with temperature decreasing.

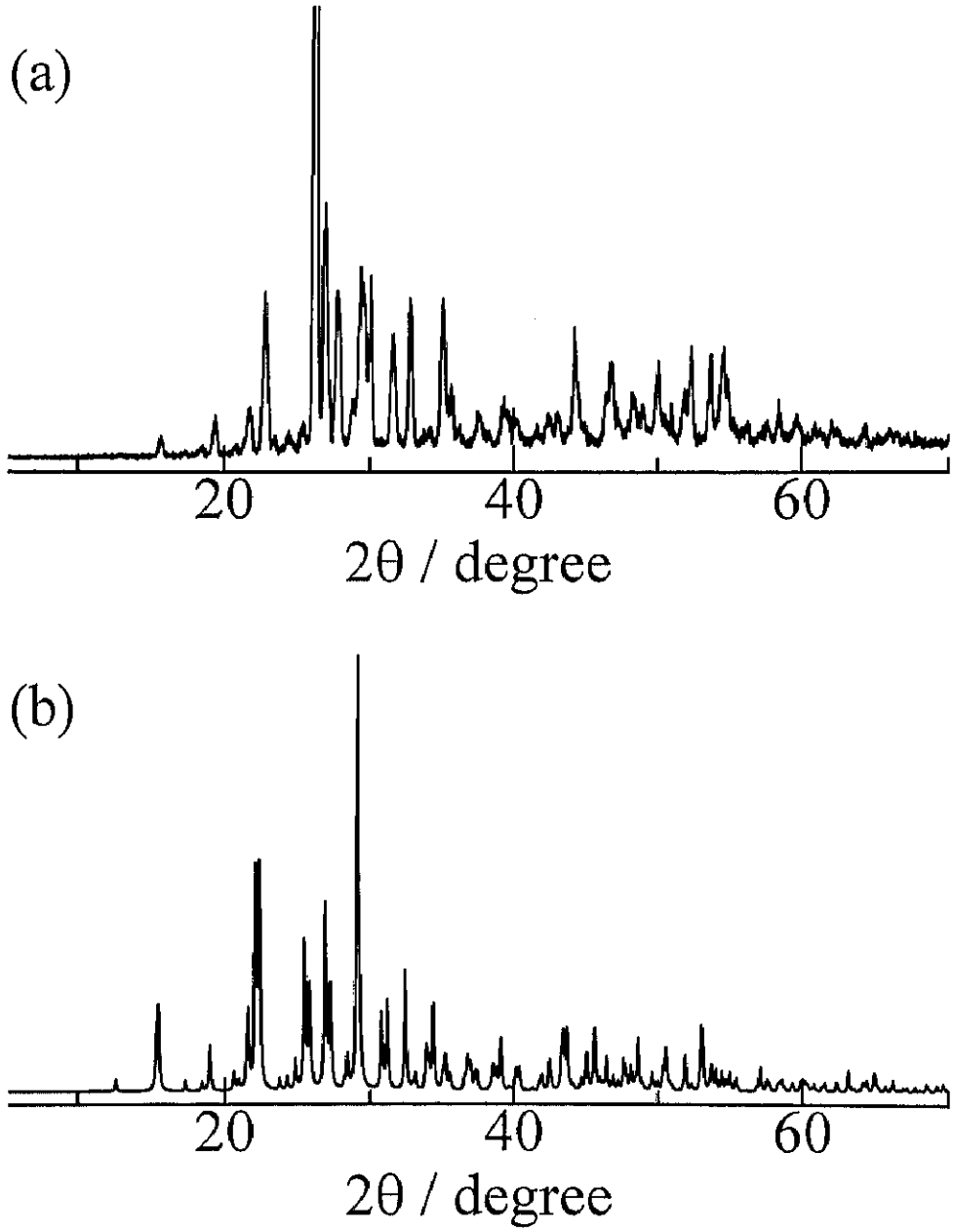

Fig. 3. 6 (a) An X-ray powder diffraction pattern observed at ca. 300 K in Cs_2ZnBr_4. (b) A simulated powder pattern using reported atomic coordinates [43].

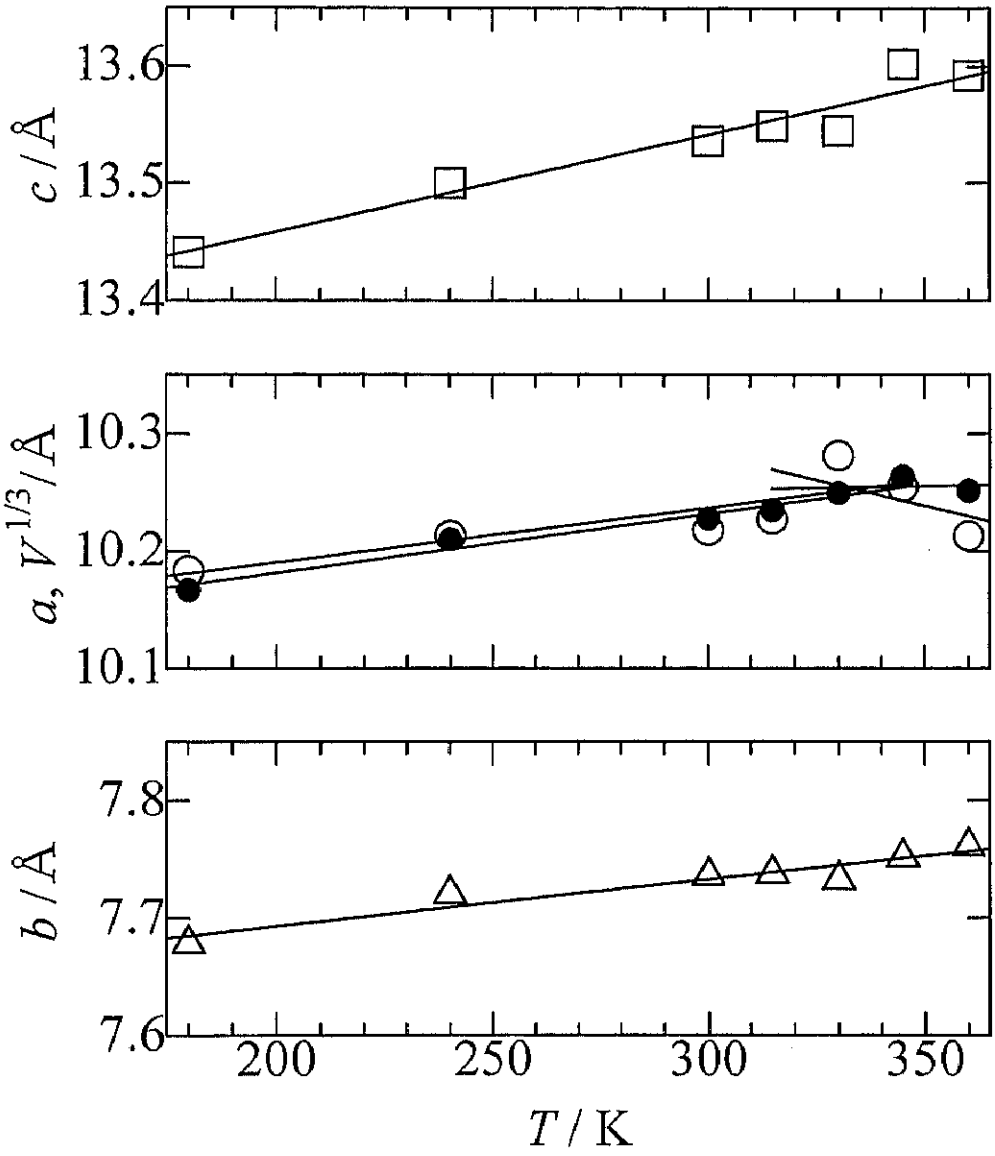

Fig. 3. 7 Temperature dependences of lattice parameters a (○), b (△) and c (□), and the cube root of a unit cell volume $V^{1/3}$ (●) in Cs_2ZnBr_4.

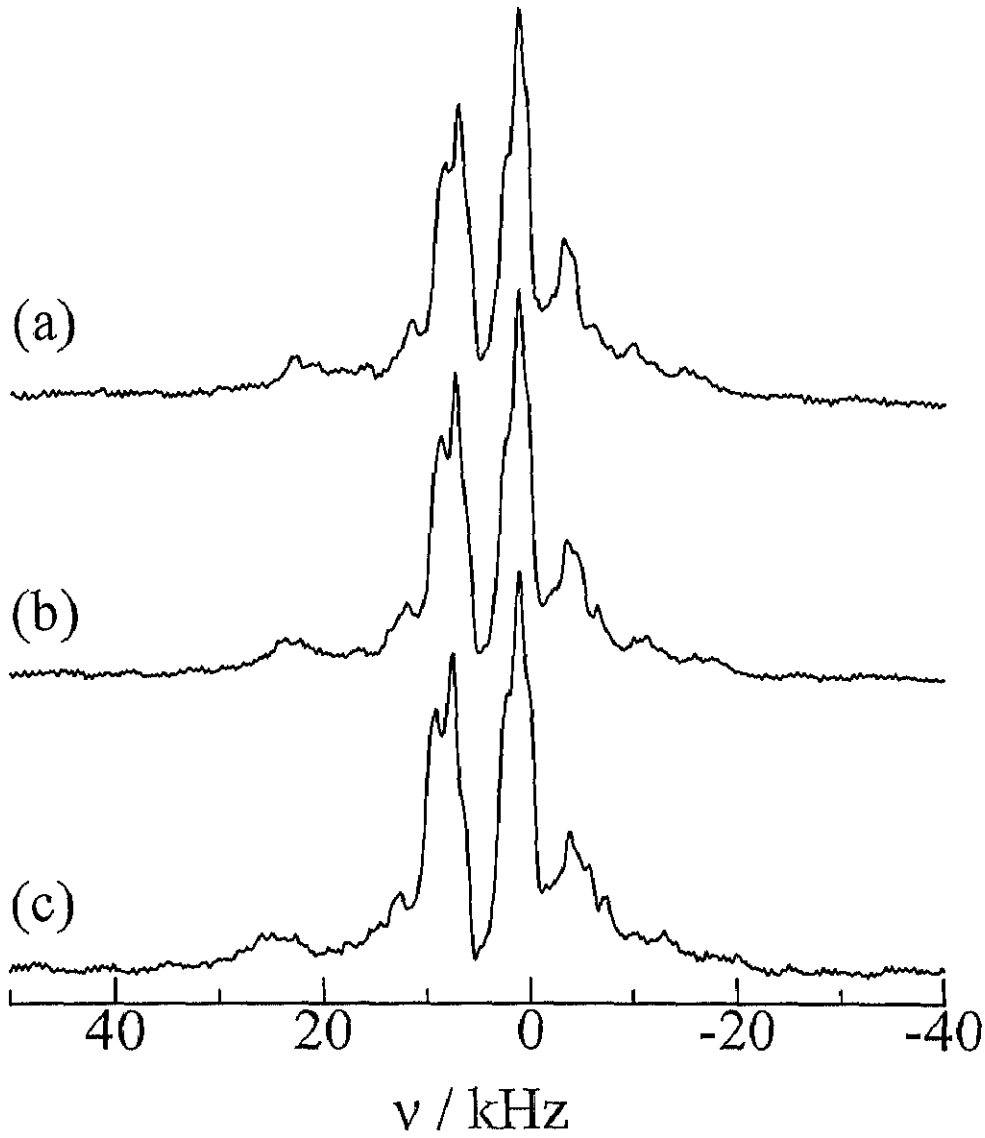

Fig. 3. 8 Quadrupolar perturbed ^{133}Cs NMR spectra measured at 39.4 MHz at 367 (a), 299 (b) and 210 K (c) in Cs_2ZnBr_4.

3.5 *Cesium tetraiodozincate Cs_2ZnI_4*

3.5.1 *Introduction*

This compound exhibits an incommensurate phase, but is assumed to be classified to the group together with Cs_2ZnCl_4 and Cs_2ZnBr_4 as an exception because the IC phase and the phase transition sequence in this compound is quite different from the group discussed in chapter 2.

Cesium tetraiodozincate Cs_2ZnI_4 forms light yellow crystals [41] and takes an orthorhombic β-K_2SO_4 structure (space group *Pnma* $Z = 4$) at room temperature [45, 46]. According to AC calorimetry [16], X-ray and ^{127}I NQR measurements [45], three thermal anomalies have been reported as the N-IC transition at $T_{IC} = 116.9$ K, the C-IC transition at $T_C = 107.58$ K and the other structural phase transition from a monoclinic commensurate to a triclinic structure at $T_{C'} = 93.77$ K. On the other hand, the adiabatic calorimetric study showed four thermal anomalies including a very small additional one at $T_{C''} = 104.44$ K [47]. The IC phase in Cs_2ZnI_4 has been characterized by the modulation wave vector $q_{IC} = (1-\delta)a^*/2$ which is 2 or 3 times larger than that in the group discussed in chapter 2. Furthermore, two different space groups, $P2_1/n$ ($Z = 8$) [45] or $P2_1/m$ ($Z = 8$) [48], were reported independently as the structure of the C phase and both structures have a two-fold superlattice along *a*-axis. These structures are also different from that in the previous compounds discussed in chapter 2. In the C' phase, the space group becomes $P\bar{1}$ ($Z = 4$) in which the unit cell volume is a half of that in the C phase, i.e., the same size as that in the N phase. Three ^{127}I NQR lines of $\pm 1/2 \Leftrightarrow \pm 3/2$ transitions with an intensity ratio 2:1:1 consistent with the crystal structure determination performed at room temperature were observed at 298 K [38]. Eight NQR

lines, which are expected to be detected in both $P2_1/n$ (Z = 8) and $P2_1/m$ (Z = 8) structures in the C phase, and $P\bar{1}$ (Z = 4) in the C' phase, were observed in a range 80 K $< T <$ 108 K [45, 49]. The phase transition at $T_{C''}$ reported by the measurement of adiabatic calorimetry [47] has not been confirmed clearly, though extensive studies of X-ray diffraction [45, 48-52], dielectric [41, 45, 53,], Raman scattering [19, 54, 55], birefringence [55-57], ^{127}I NQR [38, 45, 49, 52] and ^{133}Cs NMR spectrum [52] measurment were performed.

$T_{C'}$ = 93.8 K	($T_{C''}$ = 104.4 K)	T_C = 107.6 K	T_{IC} = 116.9 K	
commensurate	→ commensurate	→ commensurate	→ incommensurate	→ normal
$P\bar{1}$	($P\bar{1}$)	$P2_1/n$ or $P2_1/m$		*Pnma*
Z = 4	(Z = 4)	Z = 8		Z = 4

3.5.2 Experimental

Crystals of Cs_2ZnI_4 with the β-K_2SO_4 structure were grown by cooling a molten mixture containing stoichiometric amounts of CsI (purity 99.9 %) and ZnI_2 (purity 99.5 %) purchased from Wako Pure Chemical Industries, Ltd. The obtained crystalline powder was dried *in vacuo* and then sealed in glass tubes with nitrogen gas for DTA and NMR measurements.

DTA was carried out to confirm reported phase transitions in a range 90-300 K. The sample temperature was determined within $\pm$0.2 K by using a chromel-constantan thermocouple.

To confirm lattice parameters, X-ray powder diffraction was measured and their temperature dependences were obtained using a Phillips X'Pert PW3050/00

diffractometer in a range 180-360.

The ^{133}Cs NMR spectra were measured with a Bruker MSL-300 NMR system at a Larmor frequency of 39.4 MHz in a range 219-359 K. A saturated CsCl aqueous solution was used as a standard of frequency shift and the setting the pulse width. All ^{133}Cs NMR spectra were measured by applying a single detection 90° pulse with a width 4-6 μs. ^{133}Cs NMR T_1 measurements were performed with a Bruker MSL-300 NMR system at a Larmor frequency of 39.4 MHz using the saturation-τ- 90° pulse sequence in a range 204-371 K. The sample temperature was controlled within ±0.5 K with a VT-1000 temperature controller and determined by a copper-constantan thermocouple with the same accuracy. The uncertainty in the T_1 measurement was estimated to be within 5 %.

3.5.3 Result

DTA thermograms measured on heating showed endothermic anomalies due to phase transitions at 92.3±0.6 and 106.9±0.8 K in good agreement with previously reported phase transition temperatures $T_{C'}$ and T_C, respectively [16]. No thermal anomalies could, however, be detected around T_{IC} = 117 K and $T_{C''}$ = 104 K reported as very small peaks by the adiabatic calorimetry measurement [47]. The measured crystals are expected to form an N phase above 117 K.

An X-ray powder diffraction pattern recorded at *ca.* 300 K is shown in Fig. 3. 9 together with the diffraction lines calculated using atomic coordinates reported at room temperature [46]. Lattice parameters determined from the experimental pattern observed at *ca.* 300 K given below agreed well with reported values (in parentheses): a =10.81 ±

0.02 Å (10.812 Å), b =8.32±0.02 Å (8.306 Å) and c =14.39±0.03 Å (14.464 Å). Temperature dependeences of lattice parameters are shown in Fig. 3. 10. The parameter c decreases upon cooling from 360 K, while a showed a minimum at *ca.* 300 K. Temperature dependences of b and $V^{1/3}$ gave a steep decrease on cooling and a plateau above and below 300 K, respectively.

Observed quadrupolar perturbed ^{133}Cs NMR spectra are shown in Fig. 3. 11. Since a 90° pulse tured for the measurement of the powder sample had the same width as that adjusted in the standard CsCl aqueous solution, all single quantum transitions in ^{133}Cs nuclei of I = 7/2 are expected to be contained in observed ^{133}Cs NMR spectra, and ^{133}Cs nuclei in this sample can be considered to have small quadrupole coupling constants (e^2Qq/h) . The line shapes are explainable by the superposition of two 1st order perturbed spectra. e^2Qq/h and η observed at *ca.* 300 K were determined to be 140 ±30 kHz and 0.05±0.05, and 200±70 kHz and 0.5±0.2, respectively, by referring to the values obtained in a single crystal ^{133}Cs NMR measurement in Cs_2HgBr_4 [42].

The recovery of ^{133}Cs magnetization after a 90° pulse could be reproduced by a single exponential curve in the whole temperature range studied and a unique T_1 value could be determined. A temperature dependence of ^{133}Cs NMR T_1 is shown in Fig. 3. 5. The T_1 increased with the temperature decrease, and the temperature gradient became gentle below *ca.* 340 K.

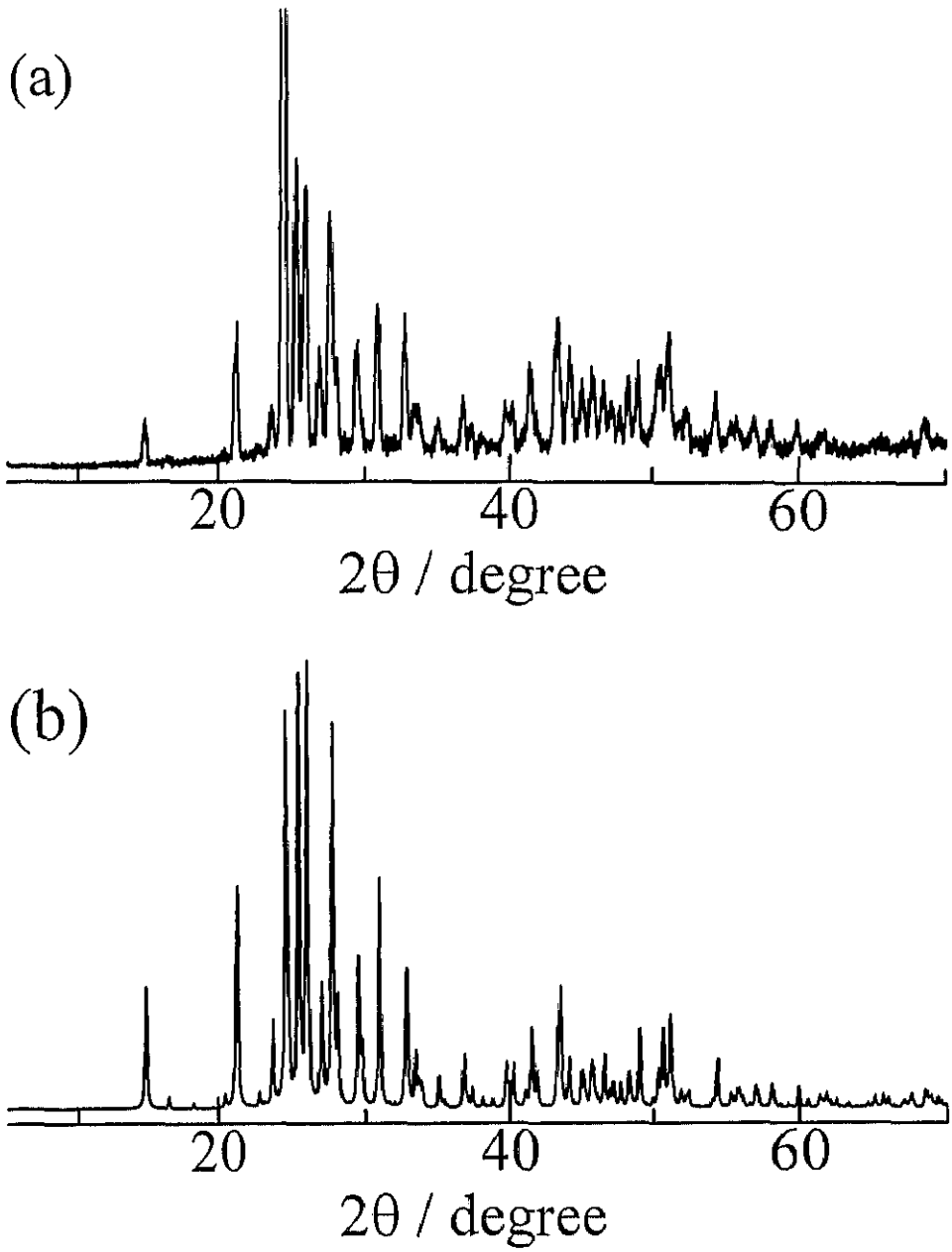

Fig. 3. 9 (a) An X-ray powder diffraction pattern observed at ca. 300 K in Cs_2ZnI_4. (b) A simulated powder pattern using reported atomic coordinates [46].

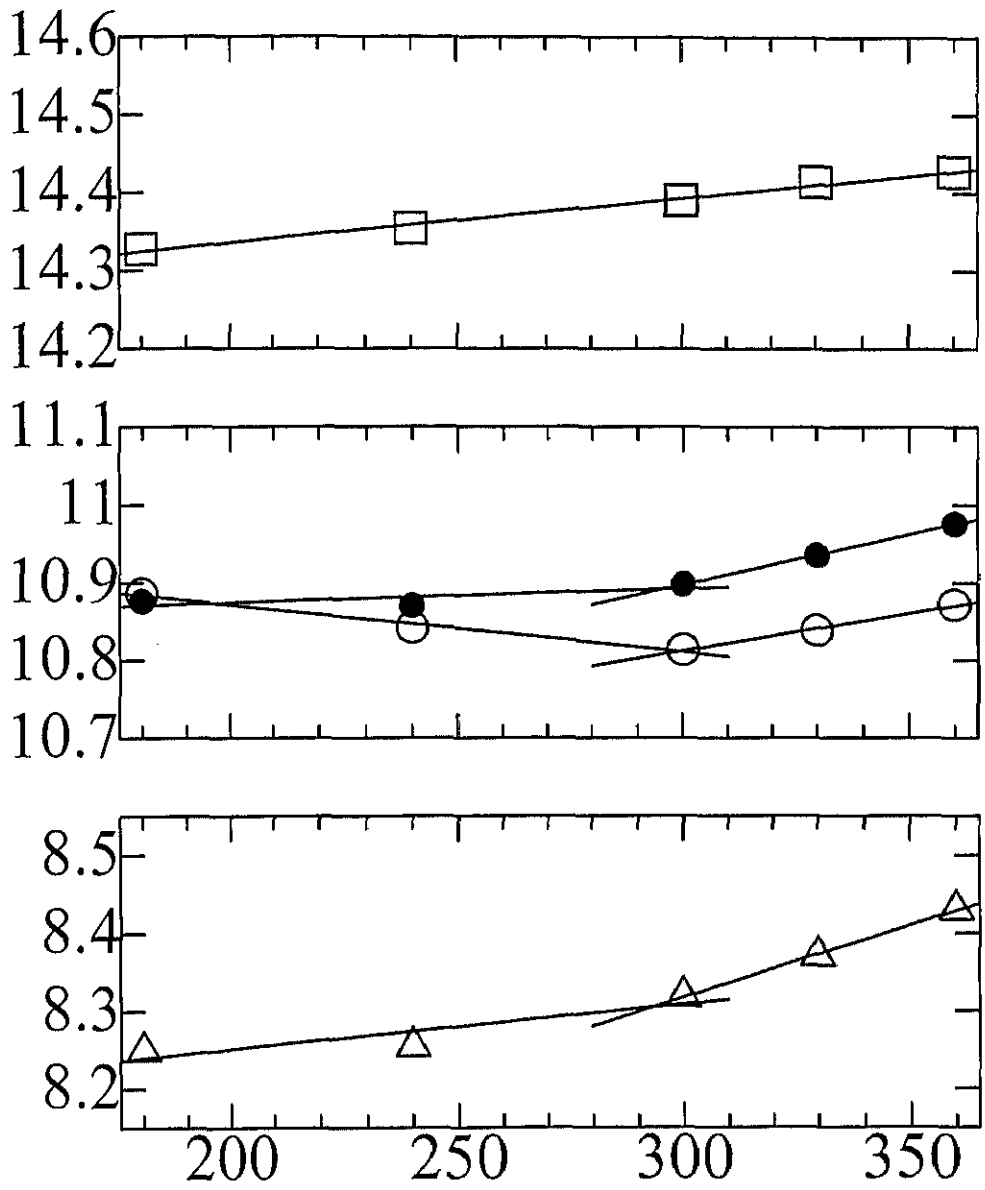

Fig. 3. 10 Temperature dependences of lattice parameters a (○), b (△) and c (□), and the cube root of a unit cell volume $V^{1/3}$ (●) in Cs_2ZnI_4.

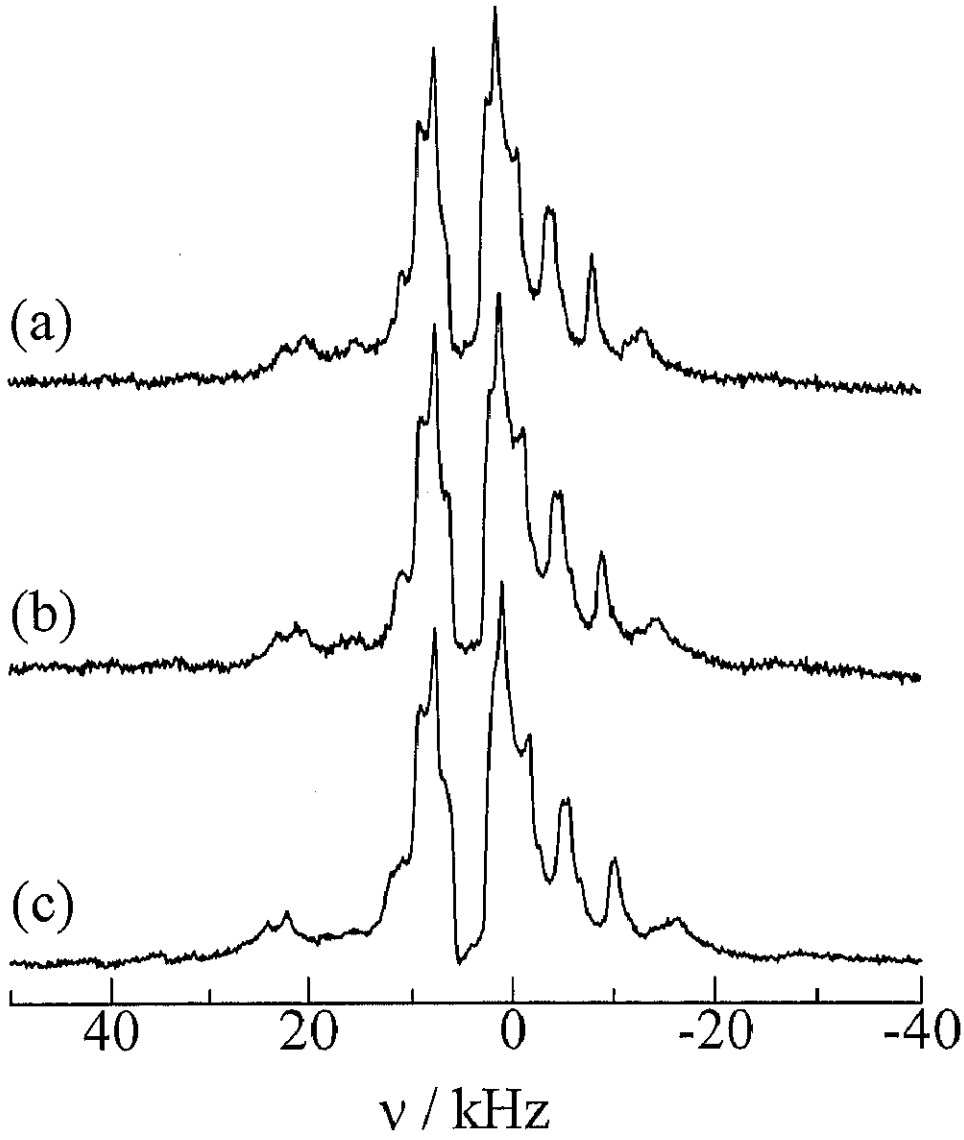

Fig. 3. 11 Quadrupolar perturbed ^{133}Cs NMR spectra measured at 39.4 MHz at 359 (a), 298 (b) and 219 K (c) in Cs_2ZnI.

3.6 *Modification-B of Cesium tetraiodocadmate Cs_2CdI_4*

3.6.1 Introduction

As mentioned in subsection 2.5.1, Cs_2CdI_4 crystals grown from the aqueous solution contain a small amount of water and take the modification-B with a monoclinic Sr_2GeS_4 structure ($P2_1/m$, Z = 4) [59, 60]. The modification-B undergoes no phase transition below room temperature. Three lines with an intensity ratio 1:2:1 which agrees with the ratio of nonequivalent I sites in the structure determined were observed between 77 and 373 K by the ^{127}I NQR measurement [8]. Upon heating, Cs_2CdI_4 crystals transform from the modification-B to -A at *ca.* 420 K [6] and melts 720 K [61].

3.6.2 Experimental

Crystalline Cs_2CdI_4 was grown from an aqueous solution using a similar manner described in Chapter 2. In this chapter, results on NMR measurements for non-annealed sample to investigate the behavior of the modification-B of Cs_2CdI_4 with the Sr_2GeS_4 structure are discussed.

DTA was carried out to confirm reported phase transitions in a range 100-360 K for the modification-B of Cs_2CdI_4. The sample temperature was determined within ± 0.2 K by using a chromel-constantan thermocouple.

To confirm lattice parameters, X-ray powder diffraction was measured and their temperature dependences were obtained using a Phillips X'Pert PW3050/00 diffractometer in a range 170-360 K for the modification-B of Cs_2CdI_4.

The ^{133}Cs NMR spectra were measured with a Bruker MSL-300 NMR system at a Larmor frequency of 39.4 MHz in a range 220-367 K for the modification-B of

Cs_2CdI_4. A saturated CsCl aqueous solution was used as the standard of frequency shift and for the setting of the pulse width. All ^{133}Cs NMR spectra were measured by applying a single detection 90° pulse with a width 4-6 μs. ^{133}Cs NMR T_1 measurements were performed with a Bruker MSL-300 NMR system at a Larmor frequency of 39.4 MHz using the saturation-τ- 90° pulse sequence in a range 220-365 K. The sample temperature was controlled within ±0.5 K with a VT-1000 temperature controller and determined by a copper-constantan thermocouple with the same accuracy. The uncertainty in the T_1 measurement was estimated to be within 5 %.

3.6.3 Result

No thermal anomaly was detected by DTA measurement below 300 K. A large anomaly, however, was observed at ca. 420K corresponding to the transition to modification-A called the α-β transition. An X-ray powder diffraction pattern observed at *ca.* 300 K for the modification-B without annealing is shown in Fig. 2. 20. Lattice parameters determined from the pattern observed at *ca.* 300 K together with the reported values [59] shown in parentheses are given by a =7.84 Å (7.838 Å), b =8.40 Å (8.403 Å), c =11.05 Å (11.048 Å) and β=110.3° (110.57°). Temperature dependences of lattice parameters for the modification-B are shown in Fig. 3. 12. Lattice parameters a, b and c and the cube root of a unit cell volume $V^{1/3}$ are slightly decreased upon cooling.

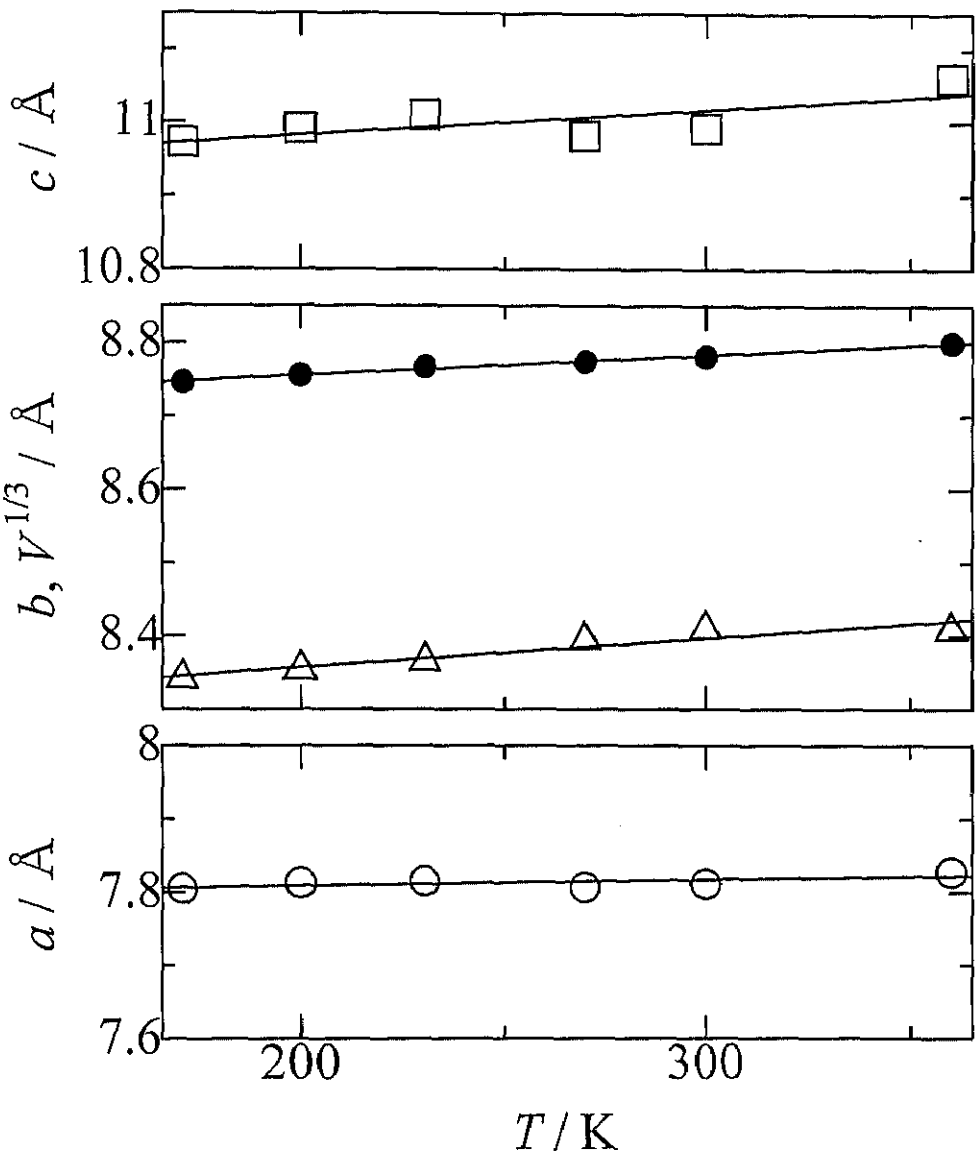

Fig. 3. 12 Temperature dependences of lattice parameters a (○), b (△) and c (□), and the cube root of a unit cell volume $V^{1/3}$ (●) in the modification-B of Cs_2CdI_4.

Quadrupolar perturbed ^{133}Cs NMR spectra are shown in Fig. 3. 13. The width of a 90° pulse tuned for the measurement of powder sample was almost the same as that adjusted to the standard CsCl aqueous solution. This suggests that all single quantum transitions were contained in observed ^{133}Cs spectra, and ^{133}Cs nuclei have small quadrupole coupling constants (e^2Qq/h). The observed line-shapes are considered to be explained by the superposition of two 1st order perturbed spectra, because of the existence of two crystallographically nonequivalent Cs ions as previously reported [59, 60].

The recovery of ^{133}Cs magnetization after a 90° pulse could be reproduced by a single exponential curve in the whole temperature range and hence T_1 could be determined. A temperature dependence of ^{133}Cs NMR T_1 is shown in Fig. 3. 5. The T_1 increased with temperature decreasing.

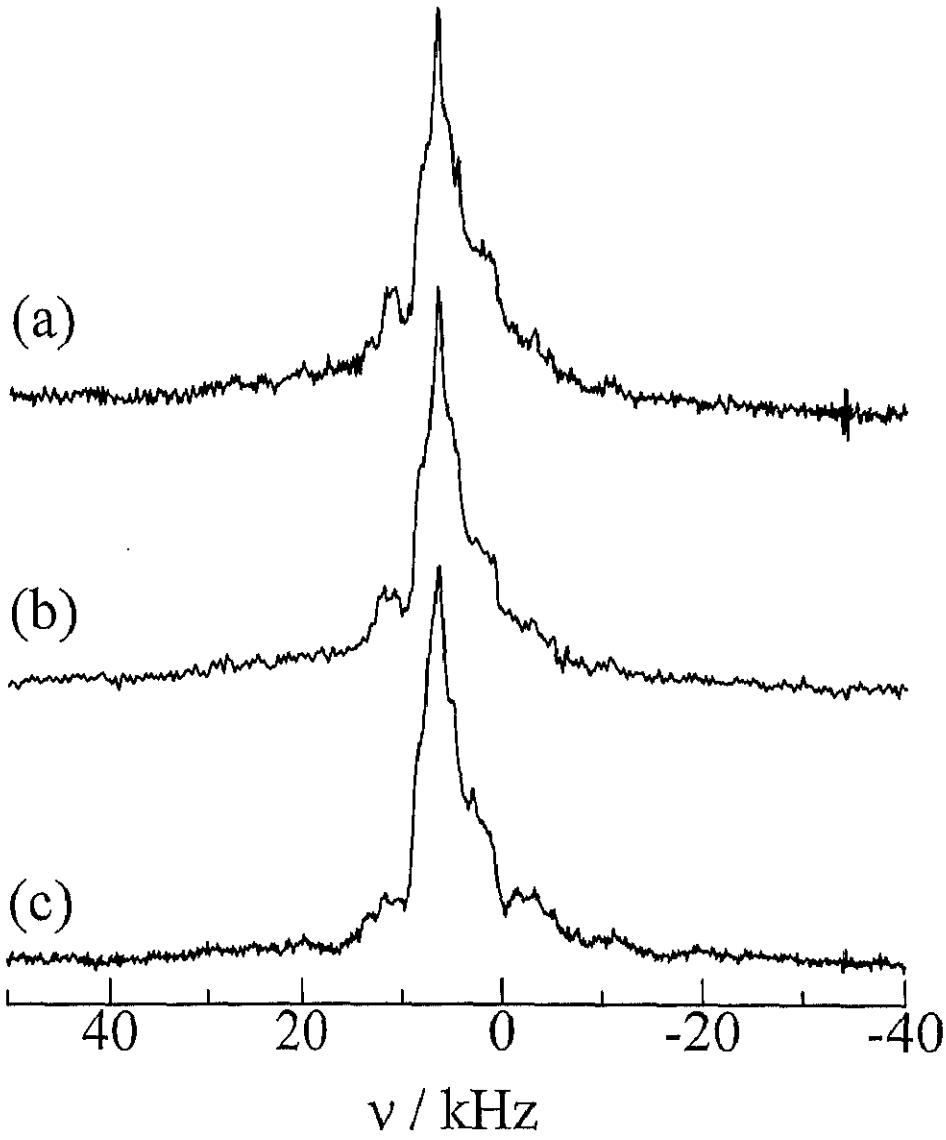

Fig. 3. 13 Quadrupolar perturbed ^{133}Cs NMR spectra measured at 39.4 MHz at 367 (a), 299 (b) and 220 K (c) in the modification-B of Cs_2CdI.

3.7 *Modification-B of cesium tetraiodomercurate Cs_2HgI_4*

3.7.1 Introduction

Crystalline cesium tetraiodomercurate Cs_2HgI_4 of modification-B is yellow and takes a monoclinic Sr_2GeS_4 structure (space group $P2_1/m$ $Z = 2$) at room temperature [62]. Dielectric constants of this compounds have been reported to increase monotonically along *b*-axis and slightly decrease along *a*-axis with temperature decrease down to the liquid helium temperature [63]. The negative Curie-Weiss temperature shown from the dielectric constant measurement along *b*-axis means that the net interaction between the molecular dipole units is antiferroelectric in the modification-B. No anomaly related to the phase transition was observed in the modification-B below 300 K [63]. On the other hand, a phase transformation to a pale red modification-A, which is considered to be a superionic state [64], has been reported at 518 K [65]. It was shown by the ^{127}I NQR measurement that the modification-A of this compound has phase transitions at 200 K and 255 K. Three and sixteen NQR lines were reported above 255 K and below 200 K, respectively [12]. The fact that NQR signals were not observed between 200 and 255 K is explainable by the appearance of an IC phase in this temperature region [12] but the phase character in the modification-A has not been investigated in detail.

3.7.2 Experimental

Crystals of Cs_2HgI_4 with the Sr_2GeS_4 structure were grown by cooling a molten mixture containing stoichiometric amounts of CsI (purity 99.9%) and HgI_2 (purity 99.9%) purchased from Wako Pure Chemical Industries, Ltd. The obtained crystalline

powder was dried *in vacuo* and then sealed in glass tubes with nitrogen gas for DTA and NMR measurements.

DTA was carried out to confirm reported phase transitions in a range 100-300 K for the modification-B of Cs_2HgI_4. Furthermore, DTA was carried out for the modification-A in the temperature range 100-350 K after the sample was put in a glass tube and kept at 550K in oil bath for 1 hour to obtained the modulation-A. The sample temperature was determined within $\pm$ 0.2 K by using a chromel-constantan thermocouple.

To confirm lattice parameters, X-ray powder diffraction was measured and their temperature dependences were obtained using a Phillips X'Pert PW3050/00 diffractometer in the ranges 180-360 K for the modification-B and 180-550 K for the modification-A after annealing at *ca.* 550 K.

The ^{133}Cs NMR spectra were measured with a Bruker MSL-300 NMR system at a Larmor frequency of 39.4 MHz in a range 214-358 K for modification-B of Cs_2HgI_4. A saturated CsCl aqueous solution was used as a standard of frequency shift and for the setting of the pulse width. All ^{133}Cs NMR spectra were measured by applying a single detection 90° pulse with a width 4-6 μs. ^{133}Cs NMR T_1 measurements were performed with a Bruker MSL-300 NMR system at a Larmor frequency of 39.4 MHz using the saturation-τ- 90° pulse sequence in a range 214-359 K for the modification-B of Cs_2HgI_4. The sample temperature was controlled within $\pm$0.5 K with a VT-1000 temperature controller and determined by a copper-constantan thermocouple with the same accuracy. The uncertainty in the T_1 measurement was estimated to be within 5 %.

3.7.3Result

No thermal anomaly was detected by DTA measurement below 300 K in the modification-B of Cs_2HgI_4. On the other hand, two phase transitions at 258.3 ±0.6 and 237.3 ±0.8 K, and another possible phase transition with a small anomaly in the noisy background were observed at 319±2 K in the modification-A observed by supercooling after annealed at *ca.* 550 K, though the modification-A was transformed into the modification-B in several hours.

X-Ray powder diffraction patterns observed at *ca.* 300 K for the modification-B without annealing together with the simulated pattern used atomic coordinates reported at room temperature [62], and for the modification-A after annealing are shown in Figs. 3. 14-15. Lattice parameters determined from the experimental pattern observed at *ca.* 300 K together with the reported values [62] shown in parentheses in the modification-B are a =7.74 Å (7.734 Å), b =8.39 Å (8.386 Å), c =11.03 Å (11.019 Å) and β=110.1° (110.06°) for the modification-B, and a =10.90 Å, b =8.30 Å and c =14.90 Å for the modification-A. The obtained parameters in the modification-B agree well with the reported values. On the other hand, the modification-A of Cs_2HgI_4 may have a symmetry higher than *Pnma*, because the number of diffraction peaks were much less than those of other Cs_2MX_4 compounds with the β-K_2SO_4 structure. Temperature dependeences of lattice parameters for the modification-B and -A are shown in Figs. 3. 16-17. For the modification-B, all parameters slightly decreased upon cooling. All parameters in the modification-A were slightly decreased above ca. 340 K, while steeply decreased below the temperature upon cooling.

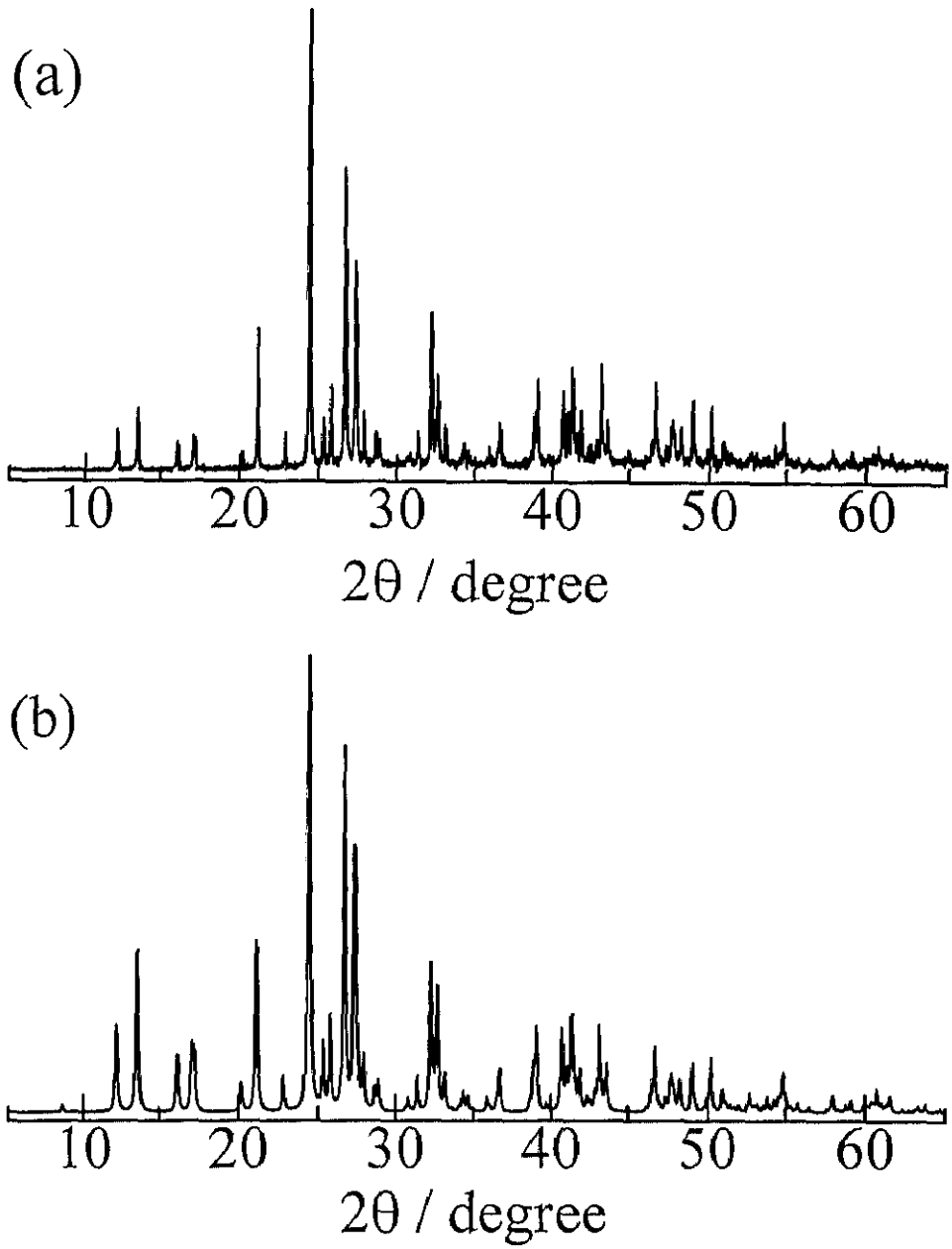

Fig. 3. 14 (a) An X-ray powder diffraction pattern observed at ca. 300 K in the modification-B of Cs_2HgI_4. (b) A simulated powder pattern using reported atomic coordinates [62].

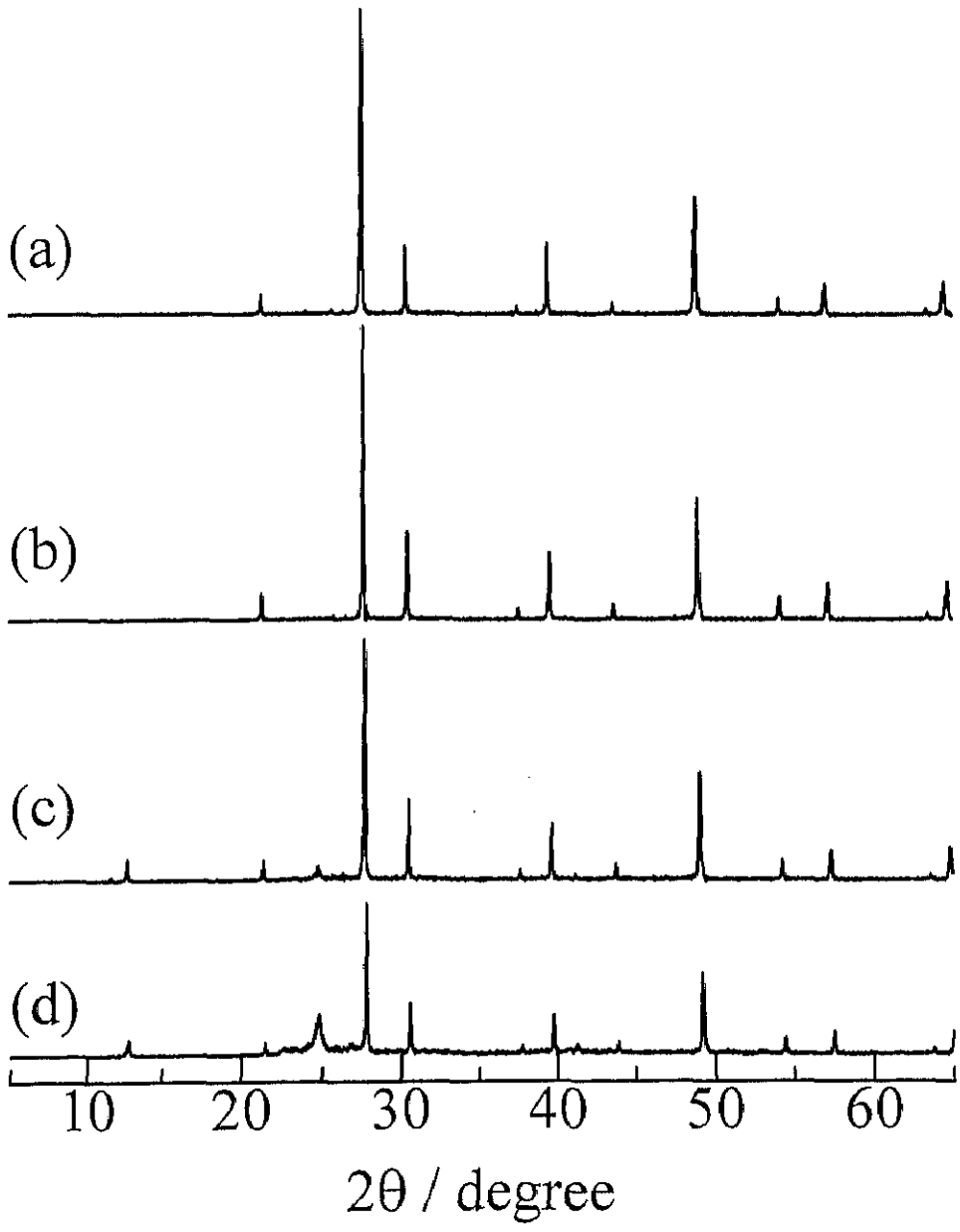

Fig. 3. 15 X-ray powder diffraction patterns observed at *ca.* 340 (a), 300 (b), 245 (c) and 180 K (d) in the modification-A of Cs_2HgI_4.

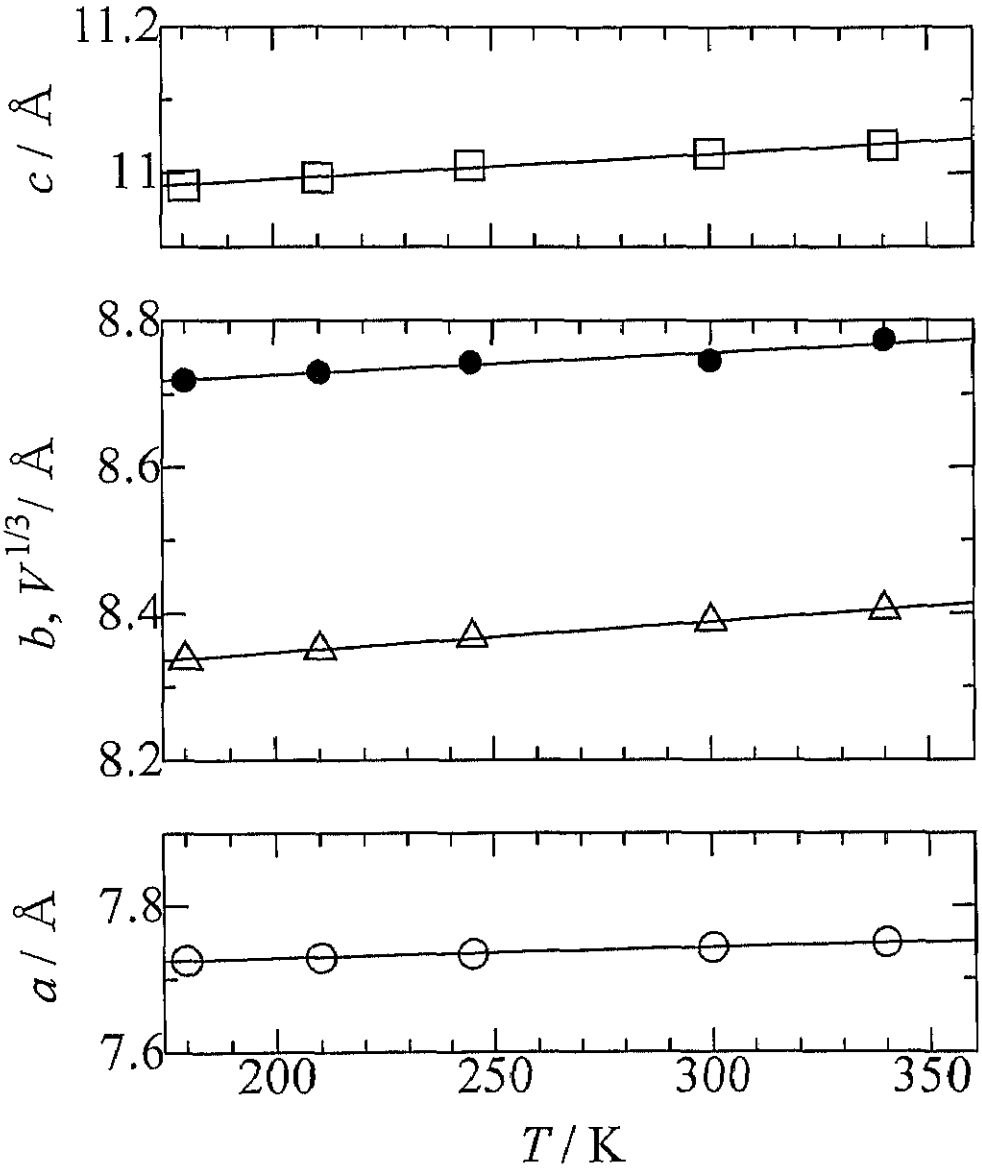

Fig. 3. 16 Temperature dependences of lattice parameters a (○), b (△) and c (□), and the cube root of a unit cell volume $V^{1/3}$ (●) in the modification-B of Cs_2HgI_4.

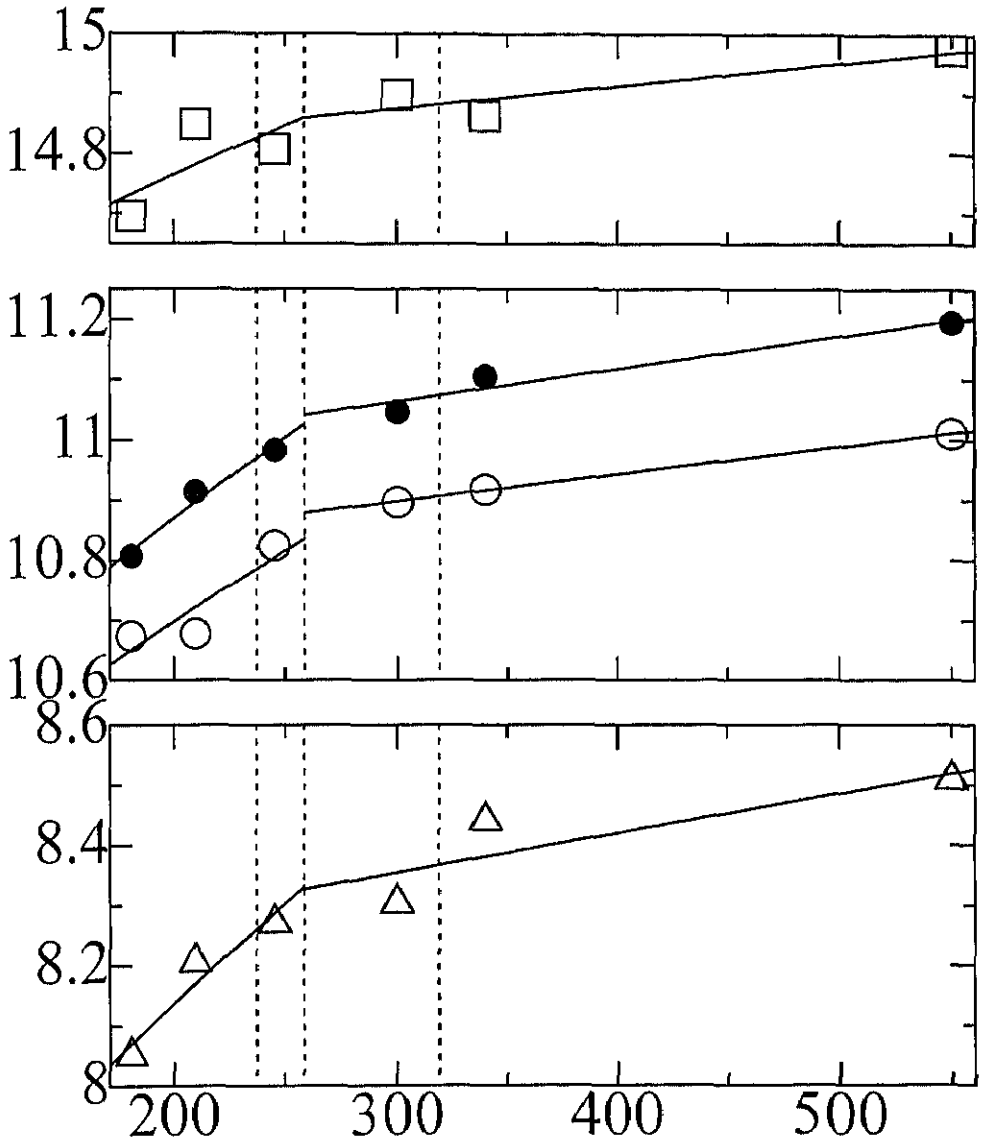

Fig. 3. 17 Temperature dependences of lattice parameters a (○), b (△) and c (□), and the cube root of a unit cell volume $V^{1/3}$ (●) in the modification-A of Cs_2HgI_4.

^{133}Cs NMR measurements of modification-A was not carried out because this modification is unstable and gradually transformed to B. Quadrupolar perturbed ^{133}Cs NMR spectra for the modification-B are shown in Fig. 3. 18. Since a 90° pulse width tuned for the measurement of powder samples was close to that for the standard CsCl aqueous solution, all single quantum transitions were assumed to be contained in observed ^{133}Cs NMR spectra indicating that ^{133}Cs nuclei have small quadrupole coupling constants (e^2Qq/h). The observed line-shapes are considered to be explained by the superposition of two 1st order perturbed spectra, because of the existence of two crystallographically nonequivalent Cs ions as previously reported [62].

The recovery of ^{133}Cs magnetization after a 90° pulse could be reproduced by a single exponential curve in the whole temperature range studied and a unique T_1 value could be determined. A temperature dependence of ^{133}Cs NMR T_1 in modification-B is shown in Fig. 3. 5. The T_1 increased with temperature decrease.

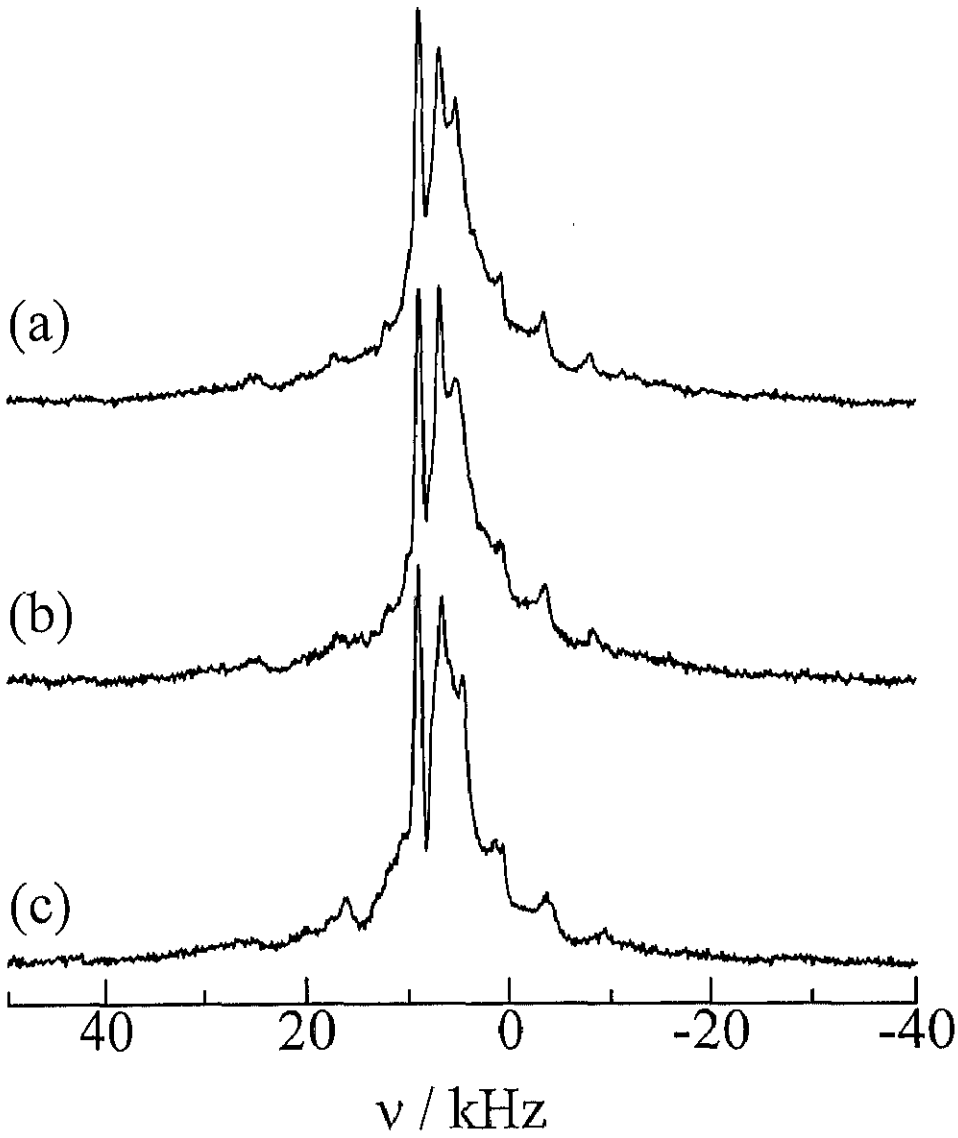

Fig. 3. 18 Quadrupolar perturbed ^{133}Cs NMR spectra measured at 39.4 MHz at 328 (a), 299 (b) and 214 K (c) in the modification-B of Cs_2HgI.

3.8 Discussion

3.8.1 Thermal expansion

Averaged coefficients of linear and cubical expansions were estimated from temperature dependences of lattice parameter using eq. (3.15)-(3.16) and are listed in Table 3.4. β-K_2SO_4- and Sr_2GeS_4-type compounds without IC phase at low-temperatures, i.e., Cs_2ZnCl_4, Cs_2ZnBr_4, and Cs_2CdI_4 and Cs_2HgI_4 of modification-B, have coefficients of linear expansion along *a*-axis $\overline{\alpha}_a$ smaller than those along other axes. In compounds with analogous crystal structure, values of thermal expansions are rapidly getting large with halogen size. Comparing them in the compounds with the same halogen I, Sr_2GeS_4-type compounds (Cs_2CdI_4 and Cs_2HgI_4 of modification-B) were shown to have thermal expansion smaller than those of the β-K_2SO_4-type (Cs_2ZnI_4 and Cs_2HgI_4 of modification-A). This result implies that lattice vibrations in Sr_2GeS_4-type structures has an anharmonicity smaller than in β-K_2SO_4-type.

Table 3. 4 Averaged coefficients of liner expansions $\overline{\alpha}_a$, $\overline{\alpha}_b$ and $\overline{\alpha}_c$ along a-, b- and c-axis and those of cubical expansion $\overline{\alpha}_v$ in Cs_2MX_4 compounds in the given temperature regions.

Compound	Structure	Temperature Region	$\overline{\alpha}_a$ / 10^{-6} K^{-1}	$\overline{\alpha}_b$ / 10^{-6} K^{-1}	$\overline{\alpha}_c$ / 10^{-6} K^{-1}	$\overline{\alpha}_v$ / 10^{-6} K^{-1}
Cs_2ZnCl_4	β-K_2SO_4	180 - 360 K	11.6	41.9	37.4	91.1
Cs_2ZnBr_4	β-K_2SO_4	180 - 330 K	45.6	51.5	61.4	147.5
		330 - 360 K	-86.4	51.5	61.4	18.5
Cs_2ZnI_4	β-K_2SO_4	180 - 300 K	-56.0	69.3	39.8	50.1
		300 - 360 K	89.6	223.7	39.8	355.2
Cs_2CdI_4	Sr_2GeS_4	170 - 360 K	10.5	47.3	31.9	94.0
Cs_2HgI_4	Sr_2GeS_4	180 - 340 K	18.6	49.8	31.5	103.4
Cs_2HgI_4	(β-K_2SO_4)	180 - 258 K	217.7	402.1	109.4	729.7
		258 - 550 K	41.7	79.5	25.7	146.6

3.8.2 ^{133}Cs NMR relaxation caused by lattice vibrations and temperature dependence of covalency

The ^{133}Cs NMR T_1 observed in the foregoing compounds can be considered to be only governed by normal lattice vibrations because they have no phase transitions. Temperature dependences of ^{133}Cs NMR T_1 were fitted by eq. (2.6) with a constant A as shown in Fig. 3. 5. The fitted curves well reproduced the experimental data obtained except for Cs_2ZnX_4 (X = Cl, Br, I). In zincates, the estimated T_1 obtained by the fitting calculation was too large comparing with the experimental data in the low-temperature region. This result is considered to suggest that A is not a constant but a function of temperature, because the other relaxation mechanisms could not be found. Temperature

dependences of A given by the relation $A(T) = T_{1/}^{-1} T^{-1}$ derived from eq. (2.6) are plotted in Fig. 3. 19. $A(T)$'s for all Cs_2ZnX_4 compounds increased exponentially with temperature decrease and that for both modification-B crystals of Cs_2CdI_4 and Cs_2HgI_4 also increased slightly upon cooling. The gradients of $A(T)$ showed various values depending upon halogens and crystal structures. Sr_2GeS_4-type compounds, i.e., Cs_2CdI_4 and Cs_2HgI_4 of modification-B, showed a very small temperature dependence, while the β-K_2SO_4-type gave large values. In Cs_2ZnBr_4, the gradient of $A(T)$ showed a characteristic temperature dependence and is very small above 330 K but large below this temperature. In Cs_2ZnI_4, $A(T)$ values are not discussed, because T_1 vales below 300 K are considered to be contains the influence of the N-IC phase transition at T_{IC} = 117 K. The temperature variation of A is considered to be derived from the fact that F_2 in eq. (2.5), which relates to from the fluctuation of electric field gradient, depends on temperature. Upon cooling to 180 K, the values of F_2 which is proportional to covalency λ', increased to 1.24, 1.26, 1.05 and 1.02 for Cs_2ZnCl_4, Cs_2ZnBr_4, and modification-Bs of Cs_2CdI_4 and Cs_2HgI_4, respectively, relative to those at 360 K. The absolute value of F_2 estimated from experimental data was larger than that the electrostatic value calculated using coordinates of counter ions, because the external charges distort the ion in question[], and the covalency given by eq. (2.3) further increases electric field gradient made by the bond electrons much closer to the nucleus in question than the interionic distance R[]. Furthermore, the F_2 induced by covalency λ' depends exponentially on R as given by eqs. (2.3) and (2.4). Thermal contractions of Cs-X distance with the temperature decrease from 360 to 180 K estimated by using relative values of F_2 at 180 K to that at 360 K and eq. (2.4) are *ca.* 0.07 Å, 0.08 Å, 0.02 Å and

0.005 Å, respectively, for Cs_2ZnCl_4, Cs_2ZnBr_4, and modification-Bs of Cs_2CdI_4 and Cs_2HgI_4 assuming that temperature variations of electric field gradient are induced only along the direction with the maximum EFG component V_{ZZ}. Thus, if the assumption that the distance dependence of F_2 is induced from only that of λ' is correct, the temperature dependences of lattice parameter can be related with $A(T)$. In fact, Cs_2CdI_4 and Cs_2HgI_4 crystals of modification-B with small thermal expansions showed small gradients of $A(T)$. For Cs_2ZnBr_4, $A(T)$ inappreciably depends on temperature in the temperature range above *ca.* 330 K with very small thermal expansion, but showed a remarkable temperature dependence in the range below *ca.* 330 K with a marked thermal expansion.

3.8.3 The total degree of covalency and chemical shifts of ^{133}Cs NMR lines

Temperature dependences of peak frequencies in ^{133}Cs NMR central lines observed in Cs_2MX_4 compounds are shown in Fig. 3. 20. The observed NMR lines showed a large anisotropy of chemical shift [42] and in the shifts also contains the second order effect of quadrupolar interaction given in eq. (3.6). The isotropic chemical shifts are obtained from peak frequencies at *ca.* 300 K by subtracting the effects of anisotropy and second order shifts estimated from the line-shape of central line and eq. (3.6), respectively, as listed in Table 3.5. Their temperature dependences are shown in Fig. 3. 21. For modification-B in Cs_2CdI_4 and Cs_2HgI_4, since the estimation of e^2Qq/h and η is difficult, 5 kHz is assumed as 2nd order perturbed shift referring to the data of other Cs_2MX_4 compounds.

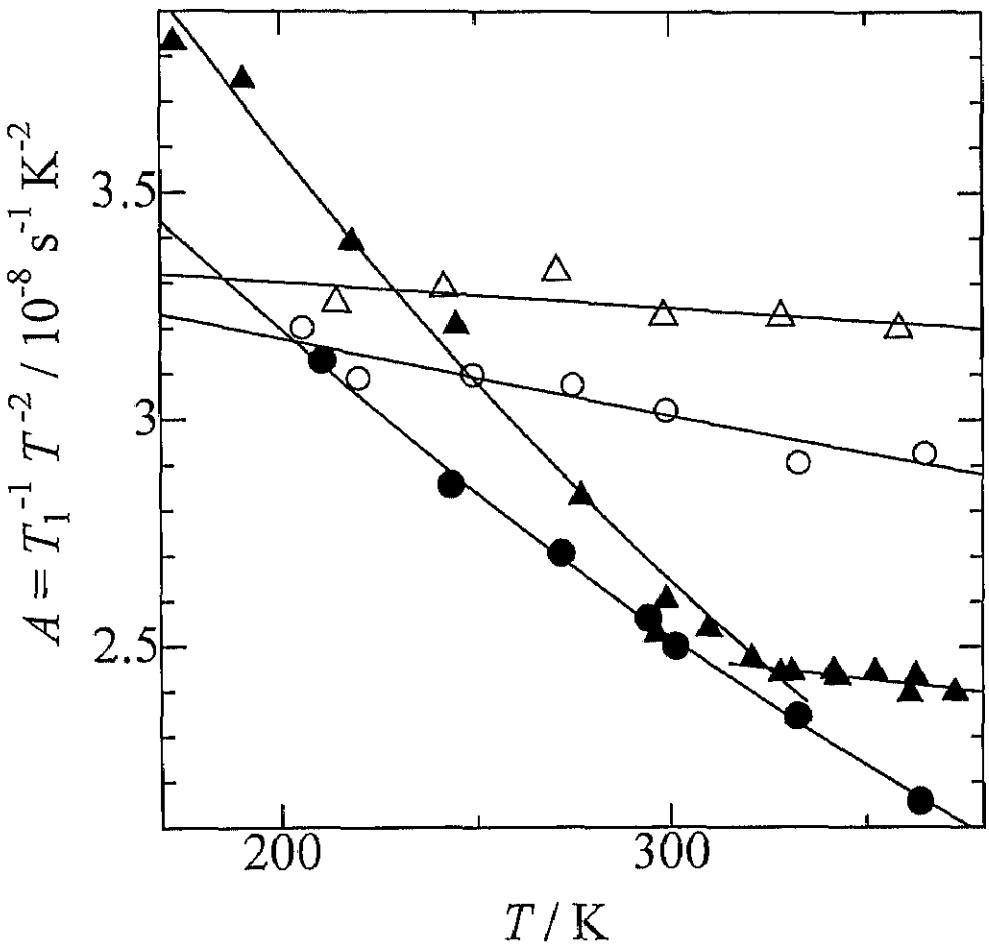

Fig. 3. 19 Temperature dependences of $A(T)$ values in eq. (2.6) obtained by substitution of ^{133}Cs NMR T_1 for Cs_2ZnCl_4 (●) and Cs_2ZnBr_4 (▲) with the β-K_2SO_4-type structure, and Cs_2CdI_4 (○) and Cs_2HgI_4 (△) with the Sr_2GeS_4-type. Solid lines are fitting curves assumed exponentially temperature dependent functions. For Cs_2ZnBr_4, the temperature dependences change drastically at about 330 K.

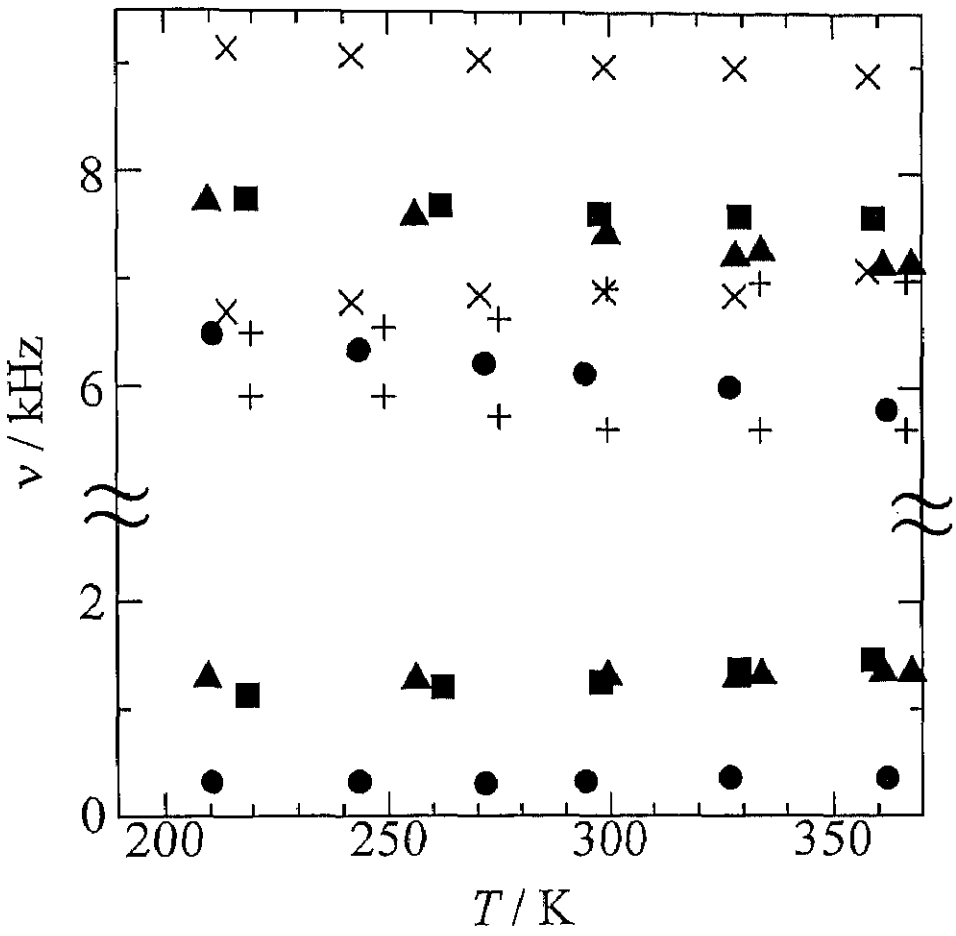

Fig. 3. 20 Temperature dependences of central peak frequencies ν in ^{133}Cs NMR spectra for Cs_2ZnCl_4 (●), Cs_2ZnBr_4 (▲) and Cs_2ZnI_4 (■) with the β-K_2SO_4-type structure, and Cs_2CdI_4 (+) and Cs_2HgI_4 (×) with the Sr_2GeS_4-type.

Table 3. 5 Chemical shifts estimated from peak frequencies after corrections of the anisotropy of chemical shifts in the central lines and the 2nd order perturbed shift derived from eq. (3.6) in Cs_2MX_4 compounds.

Compound	Peak Frequency / Hz	Frequency Correction / Hz		Chemical Shift / ppm
		Anisotropy of Chemical Shift	2nd Order Perturbed Shift	
Cs_2ZnCl_4	328	+140	+ 5	12
	6131	-300	+ 7	148
Cs_2ZnBr_4	1298	-300	+ 2	25
	7441	-400	+11	179
Cs_2ZnI_4	1252	-300	+ 3	24
	7618	+ 60	+ 7	195
Cs_2CdI_4	5911	-300	(+ 5)	143
	6918	+300	(+ 5)	183
Cs_2HgI_4	6890	± 0	(+ 5)	175
	8993	± 0	(+ 5)	228

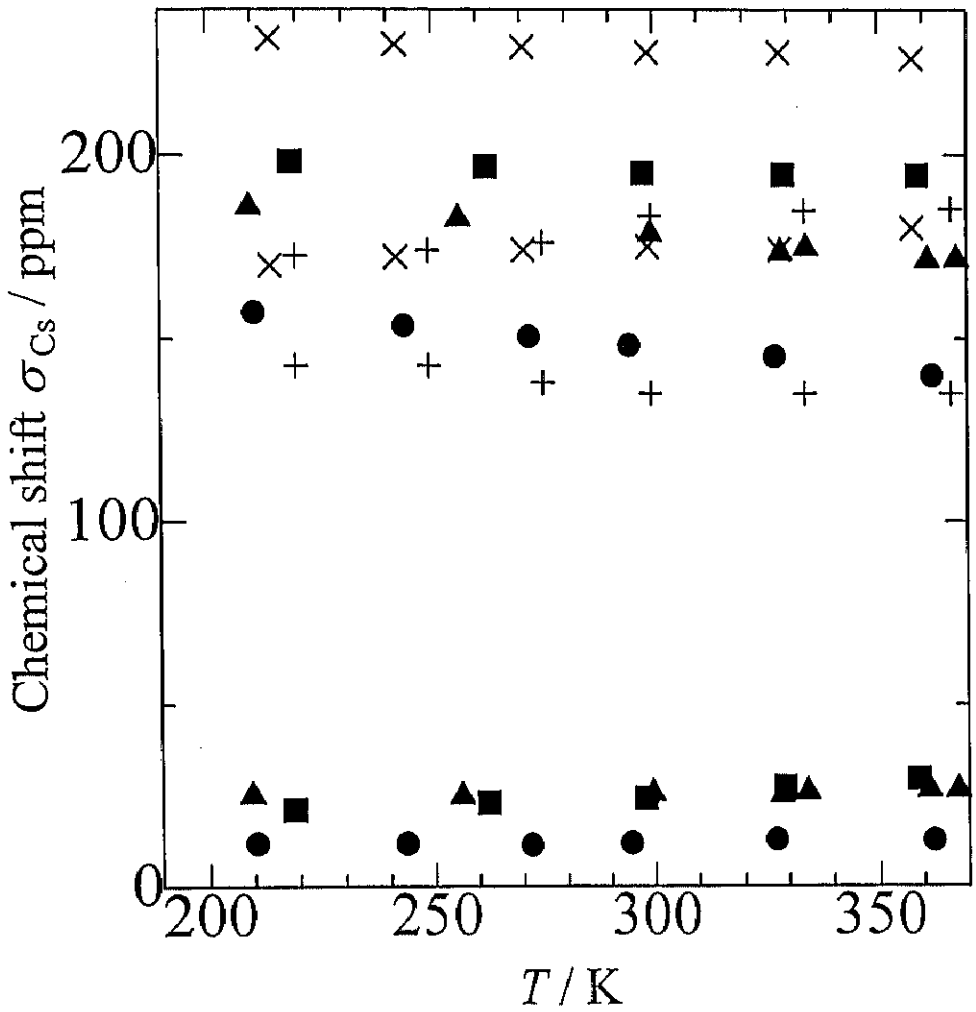

Fig 3. 21 Temperature dependences of chemical shifts observed in ^{133}Cs NMR spectra for Cs_2ZnCl_4 (●), Cs_2ZnBr_4 (▲) and Cs_2ZnI_4 (■) with the β-K_2SO_4-type structure, and Cs_2CdI_4 (+) and Cs_2HgI_4 (×) with the Sr_2GeS_4-type.

The covalency λ is estimated from the observed isotropic chemical shift and eqs. (3.11)-(3.14) and the difference of the covalency derived from the crystal structure is discussed below. The value of $\langle 1/r^3 \rangle a_0^3$ for the 5p-orbital in a Cs atom was given as 1.29 by Barnes and Smith [29] but those of 5d- and 4f-orbitals have not been known. To estimate the values of $\langle 1/r^3 \rangle a_0^3$ for 5d- and 4f-orbitals, the radial functions $R'_{n,l}(r)$ in the Slater type orbital given by

$$R'_{n,l}(r) = A_n r^{n-1} e^{-\frac{Z^* r}{n a_0}} \tag{3.19}$$

are assumed, where A_n is the normalization constant expressed by

$$A_n = \left(\frac{2Z^*}{n a_0}\right)^{n+1/2} [(2n)!]^{-1/2}, \tag{3.20}$$

and n, l, r, a_0 and Z^* are the principal and the azimuthal quantum number, the Bohr radius and the effective nuclear charge. For the 6p-orbital, if $\langle 1/r^3 \rangle a_0^3$ is equal to 1.29, Z^* takes 35.8. Since the effective nuclear charge taking into account the shielding by inner orbitals is given by $Z^* = Z' - n$ [29], 36.8 and 37.8 were used as Z^* for 5d- and 4f-orbitals, respectively. Using eq.(3.19)-(3.20) and Z^*, $\langle 1/r^3 \rangle a_0^3$ for 5d- and 4f-orbitals were estimated to be 4.43 and 20.09.

The total degrees of cavalency in cesium halides CsCl, CsBr and CsI with the CsCl structure are estimated by substituting chemical shifts reported by Gutowsky and MxGarvey [65] and ΔE values calculated by the equation applied the Born-Mayer repulsion effect to eq.(3.17) in eq. (3.11) and listed in Table 3. 6.

Table 3. 6 The degrees of covalency λ of Cs ions estimated from reported chemical shifts [65], ΔE given by eqs. (3.12)-(3.14) taking into account the Born-Mayer repulsion potential, the reported value $\langle 1/r^3 \rangle_p a_0^3$ [29] and the calculated $\langle 1/r^3 \rangle_{d,f} a_0^3$ in CsX compounds with the CsCl structure [66].

Compound	σ/ppm	ΔE / eV	$\langle 1/r^3 \rangle_p a_0^3$	$\langle 1/r^3 \rangle_d a_0^3$	$\langle 1/r^3 \rangle_f a_0^3$	λ / %
CsCl	163	8.92	1.29	4.43	20.09	32
CsBr	208	8.36	1.29	4.43	20.09	39
CsI	252	7.56	1.29	4.43	20.09	42

The degree of covalency in these compounds calculated by Pauling's [22] and Sanderson's [21] methods using the values of electronegativity are 26.6 % and 18.7 % for CsCl, 33.2 % and 23.2 % for CsBr ,and 44.5 % and 31.3 % for CsI, respectively. Degrees of covalency determined from NMR chemical shifts are consistent well with these values calculated from negativities. Therefore, the method to estimate the covalency discussed in the subsection 3.2.1 (b) is reasonable.

The total degrees of Cs covalency in Cs_2ZnCl_4, Cs_2ZnBr_4 and Cs_2ZnI_4 with the β-K_2SO_4-type structure and the modification-Bs of Cs_2CdI_4 and Cs_2HgI_4 with the Sr_2GeS_4-type structure are estimated by eq. (3.11) and listed in Table 3. 7.

Table 3. 7 The degrees of Cs covalencies λ estimated from chemical shifts, ΔE given by eqs. (3.12)-(3.14) taking into account the Born-Mayer repulsion potential and the reported values $\langle 1/r^3 \rangle_p a_0^3$ [29], and the calculated $\langle 1/r^3 \rangle_{d,f} a_0^3$ in Cs_2MX_4 compounds.

Compound	Structure	σ/ppm	ΔE / eV	λ / %
Cs_2ZnCl_4	β-K_2SO_4	12, 148	9.18	2, 24
Cs_2ZnBr_4	β-K_2SO_4	25, 179	8.54	4, 27
Cs_2ZnI_4	β-K_2SO_4	24, 195	7.66	3, 26
Cs_2CdI_4	Sr_2GeS_4	143, 183	7.44	19, 26
Cs_2HgI_4	Sr_2GeS_4	175, 228	7.47	23, 32

Consequently, we can see that one of two crytallographically nonequivalent Cs ions in Cs_2MX_4 crystals with the β-K_2SO_4-type structures has covalencies lower than in the other Cs ion of the β-K_2SO_4-type and both ions of the Sr_2GeS_4-type structures.

3.9 Conclusion

^{133}Cs NMR T_1 observed in Cs_2ZnCl_4, Cs_2ZnBr_4, Cs_2ZnI_4 with the β-K_2SO_4-type structure and Cs_2CdI_4 and Cs_2HgI_4 of the modification-B crystals with the Sr_2GeS_4-type increased with temperature decrease in the whole temperature region studied. Temperature dependences of T_1 in the Sr_2GeS_4-type compounds were explained well by the two-phonon Raman process caused by normal lattice vibrations. But temperature dependences of T_1 in Cs_2ZnCl_4 and Cs_2ZnBr_4 were unexplainable by the simple theoretical treatment of lattice mode. The deviations in the calculation from

experimental data were getting large with decreasing temperature. In Cs_2ZnI_4, influence from the low-temperature N-IC phase transition seems to be contained additionally. This is because the fluctuation of the electric field gradient relating to the relaxation is increased upon cooling. This fluctuation increase of electric field gradient can be explained by the increase of the degree of covalency in interionic bonds, which relates the shortening of interionic distance. These speculations from their temperature dependence consistent with results of thermal expansions of crystal lattice and imply that lattice vibrations in the β-K_2SO_4-type structure are more anharmonic than those in the Sr_2GeS_4-type. It was shown from ^{133}Cs NMR chemical shift measurements that one of two crytallographically nonequivalent Cs sites in Cs_2MX_4 crystals with the β-K_2SO_4-type structures has covalency lower than in the other Cs site of the β-K_2SO_4-type and both sites of the Sr_2GeS_4-type structures. These differences between A and B derived from crystal structures are considered to lead the appearance of the IC phase only in Cs_2MX_4 compounds with the β-K_2SO_4-type structure.

References in Chapter 3

[1] F. Shimizu, T. Yamaguchi, H. Suzuki, M. Takashige and S. Sawada, *J. Phys. Soc. Jpn.*, **59** (1990) 1936.

[2] F. Shimizu, H. Suzuki, M. Takashige and S. Sawada, *Ferroelectrics*, **125** (1992) 122.

[3] K. Gesi, *J. Phys. Soc. Jpn.*, **53** (1984) 3850.

[4] F. Shimizu, T. Anzai, M. Takashige and S. Sawada, *Ferroelectrics*, **168** (1995) 215.

[5] F. Shimizu and M. Takashige, *J. Kor. Phys. Soc.*, **32** (1998) S21.

[6] F. Shimizu, T. Anzai, H. Sekiguchi, M. Takashige and S. Sawada, *J. Phys. Soc. Jpn.*, **63** (1994) 437.

[7] T. Anzai, F. Shimizu, S. Sawada and M. Takashige, *J. Phys. Soc. Jpn.*, **63** (1994) 3903.

[8] E. V. Shemetov, K. S. Aleksandrov, I. P. Aleksandrova and S. V. Primak, *Phys. Stat. Sol. A*, **104** (1987) K89.

[9] K. Gesi, *J. Phys. Soc. Jpn.*, **54** (1985) 3694.

[10] F. Shimizu, S. Sawada and M. Takashige, *J. Phys. Soc. Jpn.*, **65** (1996) 870.

[11] K. S. Aleksandrov, I. N. Flerov, I. T. Kokov, A. I. Kruglik, S. V. Melnikova and E. V. Shemetov, *Ferroelectrics*, **79**, 137 (1988).

[12] A. A. Boguslavskii, D. L. Zagorskii, R. Sh. Lotfulin, V. I. Pakhomov, V. V. Kirilenko and G. K. Semin, *Russ. J. Inorg. Chem.*, **34** (1989) 1023.

[13] H. Z. Cummins, *Phys. Rep.*, **185** (1990) 211 and references therein.

[14] S. Sawada, M. Takashige, F. Shimizu, H. Suzuki and T. Yamaguchi, *Ferroelectrics*, **169**, (1995) 207.

[15] F. Shimizu, H. Suzuki, T. Yamaguchi, M. Takashige and S. Sawada, *Ferroelectrics*, **158** (1994) 181.

[16] S. N. Kallaev, A. M. Aliev, Sh. B. Abdulvagidov and A. B. Batdalov, *Phys. Solid State*, **39** (1997) 153.

[17] J. J. Melero, J. Bartolomé, R. Burriel I. P. Aleksandrova and S. Primak, *Solid State*

Commun., **95** (1995) 201.

[18] S. Plesko, P. Kind and H. Arend, *Phys. Stat. Sol. A*, **61** (1980) 87.

[19] O. P. Lamba and S. K. Sinha, *Solid State Commun.*, **57** (1986) 365.

[20] J. E. Huheey, *Inorganic chemistry, 3rd ed.*, Harper & Row, Publishers, 1983, Chap. 2.

[21] A. R. West, *Basic Solid State Chemistry*, John Wiley & Sons Ltd., 1988, Chap. 2.

[22] G. Burns, *Solid State Physics*, Academic Press, INC., 1985, Chap. 8.

[23] A. Abragam, *The Principles of Nuclear Magnetism*, Oxford University Press, Oxford, 1961, Chap. 9.

[24] T. Kanda, *J. Phys. Soc. Jpn.*, **10** (1955) 85.

[25] K. Yoshida and T. Moriya, *J. Phys. Soc. Jpn.*, **11** (1956) 33.

[26] M. H. Cohen and F. Reif, *Solid State Phys.*, **5** (1957) 321.

[27] N. F. Ramsey, *Phys. Rev.*, **78** (1950) 699.

[28] C. P. Slichter, *Principles of Magnetic Resonance, 3rd ed.*, Springer-Verlag, New York, 1990, Chap. 10.

[29] R. G. Barnes and W. V. Smith, *Phys. Rev.*, **93** (1954) 95.

[30] C. Kittel, *Introduction to Solid State Physics, 4th ed.*, John Wiley & Sons, Inc., New York, 1971, Chap. 6.

[31] *Landolt-Börnstein Zahlenwerte und Funktionen aus Physik, Chemie, Astronomie, Geophysik und Technik*, 6 Aufl., II Band, 1 Teil, S. 449 - 718, Springer-Verlab, 1971.

[32] G. A. Samara and B. Morosin, *Phys. Rev.* **B 8** (1973) 1256.

[33] H. D. Megaw, *Mat. Res. Bull.*, 6 (1971) 1007.

[34] X. Liu and R. C. Liebermann, *Phys. Chem. Miner.*, **20** (1993) 171.

[35] D. de Ligny and P. Richet, *Phys. Rev.* **B 53** (1996) 3013.

[36] G. Shirane, S. Hoshino and K. Suzuki, *Phys. Rev.*, **80** (1950) 1105.

[37] M. D. Mathews, E. B. Mirza and A.C. Momin, *J. Mater. Sci. Lett.*, **10** (1991) 305.

[38] D. E. Scaife, *Aust. J. Chem.*, **24** (1971) 1315.

[39] J. A. Mcginnety, *Inorg. Chem.*, **13** (1974) 1057.

[40] A. Onodera, O. Watanabe, H. Haga, T. Kikuta, E. Suzuki, H. Yamashita and Y. Shiozaki, *Ferroelectrics*, **125** (1992) 141.

[41] F. Shimizu, T. Anzai, S. Sawada and M. Takashige, *Ferroelectrics*, **185** (1996) 301.

[42] A. A. Boguslavskii, Yu. N. Ivanov, A. I. Krieger, A. K. Moskalev, V.I. Pakhomov and R. Sh. Lotfullin, *Phys. Stat. Sol. B*, **161** (1990) K49.

[43] B. Morosin and E. C. Lingafelter, *Acta Cryst.*, **12** (1959) 744.

[44] H. Nakayama, N. Nakamura and H. Chihara, *Bull. Chem. Soc. Jpn.*, **60** (1987) 99.

[45] I. P. Aleksandrova, S. V. Primak, E. V. Shemetov and A. I. Kruglik, *Sov. Phys. Solid State*, **33** (1991) 758.

[46] K. Friese, G. Madariaga and T. Breczewski, *Z. Kristallogr.*, **213** (1998) 591.

[47] J. Díaz-Hernández, M. J. Tello, J. M. Igartua, I. Ruiz-Larrea, T. Breczewski and A. López-Echarri, *J.Phys.: Condens. Matter*, 7 (1995) 7481.

[48] I. P. Alwksandrova, S. V. Primak, E. V. Shemetov, A. I. Kruglik and Yu. G. Elizaryev, *Ferroelectrics*, **105** (1980) 177.

[49] I.P.Aleksandrova, S.V.Primak, E.V.Shemetov, A.I.Kruglik and Yu.G.Elizaryev, *Ferroelectrics*, **105** (1990) 177.

[50] B. Sh. Bagautdinov and I. P. Aleksandrova, *Solid State Commun.*, **90** (1994) 817.

[51] B. Sh. Bagautdinov and V. Sh. Shekhtman, *Phys. Solid State*, **41** (1999) 123.

[52]

[53] K. Gesi, *J. Phys. Soc. Jpn.*, **50** (1981) 3535.

[54] O. P. Lamba, M. B. Patel, S. Ram, P. Chand and H. D. Bist, *Solid State Commun.*, **50** (1984) 321.

[55] D. P. Biliesbach and F. G. Ullman, *Ferroelectrics*, **143** (1993) 27.

[56] D. P. Billesbach and F. G. Ullman, *Rhys. Rev.* B 46 (1992) 5073.

[57] S. V. Melnikova and S. V. Primak, *Phase Transitions*, **36** (1991) 191.

[58] S. V. Mel'nikova and S. V. Primak, *Sov. Phys. Solid State*, **34** (1992) 1161.

[59] V. Touchard, M. Louër, J. P. Auffredic and D. Louër, *Rev. Chim. Min.*, **24** (1987) 414.

[60] R. Sjövall, *Acta Crystrogr. C*, **45** (1989) 667.

[61] I. N. Flerov, M. V. Gorev, L. A. Kot and V. A. Grankina, *Sov. Phys. Solid State*, **30**, (1988) 1125.

[62] R. Sjövall and C. Svensson, *Acta Crystrogr. C*, 44 (1988) 207.

[63] K. Gesi, *Jpn. J. Appl. Phys. Suppl.*, 24, (1985) 387.

[64] R. L. Ammlung, R. P. Scaringe, J. A. Ibers, D. F. Shriver and D. H. Whitmore, *J. Solid State Chem.*, **29** (1979) 401.

[65] H. S. Gutowsky and B. R. McGarvey, *J. Chem. Phys.*, 21 (1953) 1423.

[66] W. G. Wyckoff, *Crystal Structures, 2nd ed., Vol. 1*, Jon Wiley & Sons, New York, 1963, Chap. 3.